EUROPEAN ORGANIZATION FOR NUCLEAR RESEARCH (CERN)

CERN-EP-2024-088
2024/05/28

CMS-HIG-20-002

Search for a standard model-like Higgs boson in the mass range between 70 and 110 GeV in the diphoton final state in proton-proton collisions at $\sqrt{s} = 13$ TeV

The CMS Collaboration*

Abstract

The results of a search for a standard model-like Higgs boson decaying into two photons in the mass range between 70 and 110 GeV are presented. The analysis uses the data set collected by the CMS experiment in proton-proton collisions at $\sqrt{s} = 13$ TeV corresponding to integrated luminosities of 36.3 fb^{-1}, 41.5 fb^{-1} and 54.4 fb^{-1} during the 2016, 2017, and 2018 LHC running periods, respectively. No significant excess over the background expectation is observed and 95% confidence level upper limits are set on the product of the cross section and branching fraction for decays of an additional Higgs boson into two photons. The maximum deviation with respect to the background is seen for a mass hypothesis of 95.4 GeV with a local (global) significance of 2.9 (1.3) standard deviations. The observed upper limit ranges from 15 to 73 fb.

Submitted to Physics Letters B

*See Appendix A for the list of collaboration members

1 Introduction

In the standard model (SM) of particle physics [1–3], the masses of fundamental particles arise from the spontaneous breaking of electroweak symmetry, in the manner of the Brout–Englert–Higgs mechanism [4–9]. In its minimal version, this mechanism introduces a doublet of complex scalar fields. After symmetry breaking, only one scalar field remains, giving rise to the physical Higgs boson, that is experimentally observable. In 2012, the ATLAS [10] and CMS [11, 12] Collaborations observed a new boson with a mass of approximately 125 GeV whose properties are at present compatible, within uncertainties [13, 14], with those of the SM Higgs boson. The analyses of data in the diphoton final state leading to this discovery probed an invariant mass range extending from 110 to 150 GeV.

Several models for physics beyond the SM (BSM) typically contain multiple scalars with one of them being compatible with the observed 125 GeV boson. The extended parameter space of several BSM models, for example, generalized models containing two Higgs doublets (2HDM) [15–19], the next-to-minimal supersymmetric model (NMSSM) [20–40], and Georgi–Machacek models [41–44], gives rise to rich and interesting phenomenology, including the presence of additional scalars, some of which could have masses below 125 GeV. Such models provide good motivation for extending searches for additional Higgs bosons with masses m_{H} as far below 110 GeV as possible, where H refers to an additional Higgs boson that could also be "SM-like", meaning that the relative contributions of the production and decay processes are similar to those of the SM.

The $\mathrm{H} \to \gamma\gamma$ decay channel provides a clean final-state topology that allows the mass of a Higgs boson to be reconstructed with high precision. The primary production mechanism for SM-like Higgs bosons in proton-proton (pp) collisions at the CERN LHC is gluon fusion (ggH), with smaller contributions from vector boson fusion (VBF) and production in association with a W or Z boson (VH), or with a $\mathrm{t\bar{t}}$ pair ($\mathrm{t\bar{t}H}$). The dominant sources of background are irreducible direct diphoton production, and the reducible $\mathrm{pp} \to \gamma + \text{jet}$ and $\mathrm{pp} \to \text{jet} + \text{jet}$ processes, where the jets are misidentified as isolated photons. An additional source of reducible background relevant for the search range $m_{\mathrm{H}} < 110$ GeV is Drell–Yan (DY) dielectron production, where electrons might be misidentified as isolated photons.

The CERN LEP collaborations [45], in the context of the search for the SM Higgs boson, extensively explored the mass range below 110 GeV in the VH production modes, in the $\mathrm{b\bar{b}}$ and $\tau^-\tau^+$ channels. Several of the BSM models mentioned above permit a significant region of parameter space for enhanced decay rates in the diphoton channel compatible with the LEP constraints. The "low-mass" search in the diphoton decay channel by ATLAS [46], performed in the diphoton invariant mass ($m_{\gamma\gamma}$) range of $65 < m_{\gamma\gamma} < 110$ GeV at a center-of-mass energy of 8 TeV, found no significant excess of events. A CMS search [47] performed at center-of-mass energies of 8 (13) TeV in the mass ranges of $80\,(70) < m_{\gamma\gamma} < 110$ GeV reported an excess with respect to the SM background expectation, maximal for a mass hypothesis of 95.3 GeV, with a local (global) significance of 2.8 (1.3) standard deviations.

This Letter presents an update of the CMS search in the diphoton channel for an additional Higgs boson in the invariant mass range $70 < m_{\gamma\gamma} < 110$ GeV; the natural width of this additional Higgs boson is small compared to the detector resolution. The search is performed with a data set collected in 2016, 2017, and 2018 with the CMS detector at the LHC, corresponding to integrated luminosities of 36.3 fb^{-1}, 41.5 fb^{-1}, and 54.4 fb^{-1}, respectively, at a center-of-mass energy of 13 TeV. As part of this study, the data set of 2016, used in Ref. [47], has been reanalyzed with an improved detector calibration. The tabulated results are provided as HepData records [48].

The analysis is based on a search for a localized excess in the diphoton invariant mass spectrum. We follow the method used in Ref. [47], which is an extended version of the method developed for the observation and the measurement of the properties of the 125 GeV boson [49, 50]. The principal challenges associated with a search in the diphoton decay channel in the explored mass range are the ability to trigger on events while maintaining acceptable rates, and the background from Z bosons decaying to electron pairs that, through misidentification, could appear as two isolated photons. With respect to Ref. [47], additional requirements have been introduced to further discriminate against these surviving electron pairs. To achieve the best possible sensitivity, the events are separated into classes, including, for the data sets collected in 2017 and 2018, a class requiring the presence of additional jets targeting the VBF production mode. Multivariate analysis (MVA) techniques are used both for photon identification and event classification, and the signal is extracted from the background using a parametric fit to the diphoton mass spectrum in all event classes.

2 The CMS detector

A detailed description of the CMS detector, together with a definition of the coordinate system used and the relevant kinematic variables, can be found in Ref. [51]. The central feature of the CMS apparatus is a superconducting solenoid of 6 m internal diameter, providing a magnetic field of 3.8 T. Within the solenoid volume are a silicon pixel and strip tracker, a lead tungstate crystal electromagnetic calorimeter (ECAL), and a brass and scintillator hadron calorimeter (HCAL), each composed of a barrel and two endcap sections. Forward calorimeters extend the pseudorapidity (η) coverage provided by the barrel and endcap detectors. Muons are reconstructed in gas-ionization chambers embedded in the steel flux-return yoke outside the solenoid. The ECAL, surrounding the tracker volume, consists of 75 848 lead tungstate crystals, which provide coverage in $|\eta| < 1.48$ in a barrel region (EB) and $1.48 < |\eta| < 3.0$ in two endcap regions (EE). Preshower detectors consisting of two planes of silicon sensors interleaved with a total of $3X_0$ of lead are located in front of each EE detector. In the EB, an energy resolution of about 1% is achieved for unconverted or late-converting photons in the tens of GeV energy range. The energy resolution of the remaining barrel photons is about 1.3% up to $|\eta| = 1$, changing to about 2.5% at $|\eta| = 1.4$. In the EE, the energy resolution is about 2.5% for unconverted or late-converting photons, and between 3 and 4% for the other ones [52]. The diphoton mass resolution, as measured in $\mathrm{H} \to \gamma\gamma$ decays, is typically in the 1–2% range, depending on the measurement of the photon energies in the ECAL and the topology of the photons in the event [53].

The particle-flow algorithm [54] aims to reconstruct and identify each individual particle in an event, with an optimized combination of information from the various elements of the CMS detector. The energy of photons is obtained from the ECAL measurement. The energy of electrons is determined from a combination of the electron momentum at the primary interaction vertex as determined by the tracker, the energy of the corresponding ECAL cluster, and the energy sum of all bremsstrahlung photons spatially compatible with originating from the electron track. The energy of muons is obtained from the curvature of the corresponding track. The energy of charged hadrons is determined from a combination of their momentum measured in the tracker and the matching ECAL and HCAL energy deposits, corrected for the response function of the calorimeters to hadronic showers. Finally, the energy of neutral hadrons is obtained from the corresponding corrected ECAL and HCAL energies.

3 Event reconstruction, selection and categorization

3.1 Trigger and simulation

Events of interest are selected using a two-tiered trigger system. The first level, composed of custom hardware processors, uses information from the calorimeters and muon detectors to select events at a rate of around 100 kHz within a fixed latency of about 4 μs [55]. The second level, known as the high-level trigger (HLT), consists of a farm of processors running a version of the full event reconstruction software optimized for fast processing, and reduces the event rate to around 1 kHz before data storage [56].

For this analysis, diphoton HLT paths with asymmetric photon transverse momentum (p_T) thresholds, 30 and 18 GeV, are used for the data of all three years. For the 2016 data, two paths are used: one path has nearly identical requirements to those used in Ref. [50], except that only events with both photon candidates in the EB are selected. This path requires each of the photon candidates to satisfy criteria on the maximum value of the ratio of its energy in the HCAL to its energy in the ECAL (H/E), and on either the compatibility of its shower shape with that of a photon, or on the maximum value of its isolation energy [57]. The other path selects events with photon candidates from any part of the ECAL, but they must satisfy more stringent shower shape requirements, as well as the requirements on both isolation energy and H/E. Both paths impose a veto on the presence of hits compatible with the photon direction in the silicon pixel detector, and require that the invariant mass of the two photon candidates be greater than 55 GeV.

For the other two years of data taking, only one path, a relaxed variant of the latter path above, is used: for the 2017 data, at least one of the two photon candidates must satisfy the more stringent shower shape requirements, and for the 2018 data, the more stringent shower shape requirements are applied to all photon candidates in the EE, enabling the removal of the silicon pixel detector hit veto and invariant mass requirements. However, the 2018 version of the path was not introduced until after the start of that year's data taking, resulting in a reduction of the data set by approximately 5 fb^{-1}.

These HLT requirements impose a diphoton invariant mass value of $m_{\gamma\gamma} = 70$ GeV as the lower limit of the search range; this value lies above the portion of the offline diphoton spectrum that is distorted due to turn-on effects from the HLT criteria. The trigger efficiency is measured using $Z \to e^+e^-$ events and the "tag-and-probe" technique [58], except for the pixel detector hit veto requirement implemented for the triggering of the 2016 and 2017 data; the efficiency of this veto requirement is measured using diphoton events that have passed a diphoton trigger that does not require a pixel hit veto. A gradual shift in the timing of the inputs of the ECAL portion of the first level of the trigger system in the region at $|\eta| > 2.0$ caused a specific trigger inefficiency during the 2016 and 2017 data taking, affecting photons and, to a greater extent, jets [55].

Monte Carlo (MC) simulations are used to produce SM-like Higgs boson events from all production processes (ggH, VBF, VH, and $t\bar{t}H$), with Higgs boson masses ranging from 70 to 110 GeV in steps of 5 GeV. These events are the input to the signal modeling procedure, representing a new resonance decaying to two photons. They are generated at next-to-leading order (NLO) in perturbative quantum chromodynamics (QCD) using MADGRAPH5_aMC@NLO 2.4.2 [59] with FxFx merging [60] and the NNPDF3.0 [61] (NNPDF3.1 [62]) set of parton distribution functions (PDFs) to simulate the 2016 (2017 and 2018) data. Events produced via the ggH process are weighted as a function of the Higgs boson p_T and the number of jets in the event to match the prediction from the NNLOPS program [63]. The parton-level sam-

ples are interfaced with PYTHIA 8.226 (8.230) [64] for parton showering and hadronization in the simulation of the 2016 (2017 and 2018) data, with the CUETP8M1 [65] (CP5 [66]) tune parameter set used for the underlying event activity. The cross sections and branching fractions recommended by the LHC Higgs cross section working group for a center-of-mass energy of 13 TeV [67] are used for modeling the signal. After the generation step, the events are processed by the full CMS detector simulation based on GEANT4 [68]. Multiple pp interactions in each bunch crossing (pileup) are simulated. The events are weighted to reproduce the distribution of the number of interactions observed in data, the average value of which was 23 in 2016 and 32 for both 2017 and 2018. The trigger efficiencies measured using the method described above are applied to the simulated SM Higgs boson events as a correction, and the associated statistical and systematic uncertainties are propagated to the expected signal yields.

Events corresponding to the SM background processes mentioned in Section 1 are simulated using various generators. The diphoton background is modeled with the SHERPA 2.2.4 [69] generator; it includes tree-level diagrams with up to 3 additional jets, as well as box diagrams at leading order (LO). Multijet and $\gamma +$ jet backgrounds are modeled at LO with PYTHIA 8.226 (PYTHIA 8.230) for the simulation of the 2016 (2017 and 2018) data, with a filter [49, 50] applied at generator level in order to enhance the production of jets with a large fraction of electromagnetic energy. DY events are simulated at NLO with MADGRAPH5_aMC@NLO 2.4.2. All background events are generated using the same PDF sets and simulated under the same conditions as the SM-like Higgs boson events described above. The simulated background samples are used in the calculation of corrections and efficiencies, training and validation of the multivariate boosted decision trees (BDTs) used in the analysis, and in estimations of systematic uncertainties. In particular, the DY events are used for modeling the background contribution from dielectron decays of the Z boson. As in Refs. [49, 50], the background estimation is based on data.

3.2 Photon and jet reconstruction

The determination of the primary vertex from which the two photons originate has a direct impact on the diphoton invariant mass resolution. If the position along the beam axis (z) of the interaction producing the diphoton is known to better than approximately 10 mm, the invariant mass resolution is dominated by the photon energy resolution. The diphoton vertex identification method is the same as in Ref. [50]. A BDT is used to select a diphoton vertex from the set of all reconstructed primary vertices, incorporating as input variables the sum of the squared transverse momenta of the charged particle tracks associated with the vertex, and two variables that quantify the vector and scalar balance of p_{T} between the diphoton system, and the charged particle tracks associated with the vertex. Furthermore, if either photon is associated with any charged particle tracks that have been identified as resulting from conversion, the pull between the longitudinal positions of the primary vertex obtained from the conversion tracks alone and from all associated tracks is added to the BDT input variable set, as well as the number of conversions.

The photon reconstruction algorithm is the same as used in Refs. [50, 57]. Photon candidates are reconstructed by the particle-flow algorithm [54]. First, cluster "seed" crystals are identified as local energy maxima in the ECAL above a given threshold. Second, clusters are grown from the seeds by aggregating crystals with at least one side in common with a clustered crystal and with an energy in excess of a certain threshold. The energy of each crystal can be shared among adjacent clusters assuming a Gaussian transverse profile of the electromagnetic shower. Finally, clusters are merged into extended clusters or groups of clusters known as "superclusters".

The energy of a photon is computed from the sum of the energy of the clustered crystals, calibrated and corrected for changes in the ECAL response over time [70]. The preshower energy is added to that of the superclusters in the region covered by this detector. To optimize the resolution, the photon energy is corrected for the containment of the electromagnetic shower in the superclusters and the energy losses from converted photons. The correction is computed with a multivariate regression technique [52, 57] that estimates simultaneously the energy of the photon and its uncertainty. This regression is trained on simulated photons using the ratio of the true photon energy and the sum of the energy of the clustered crystals as the criterion for optimization. The inputs are shower shapes and position variables—both sensitive to shower containment and possible unclustered energy—preshower information, and global event observables sensitive to pileup.

Hadronic jets are clustered from particles reconstructed via the particle-flow algorithm [54] using the infrared- and collinear-safe anti-k_T algorithm [71, 72], with a distance parameter of 0.4. Jet momentum is determined as the vectorial sum of all particle momenta in the jet, and is found from simulation to be, on average, within 5 to 10% of the true momentum over the whole p_T spectrum and detector acceptance. Additional pp interactions within the same or nearby bunch crossings can contribute additional tracks and calorimetric energy depositions, increasing the apparent jet momentum. To mitigate this effect, tracks identified to be originating from pileup vertices are discarded and an offset correction is applied to correct for remaining contributions [73]. Jet energy corrections are derived from simulation studies so that the average measured energy of jets becomes identical to that of particle-level jets. In situ measurements of the momentum balance in dijet, photon + jet, Z + jet, and multijet events are used to determine any residual differences between the jet energy scale in data and in simulation, and appropriate corrections are made [74]. Additional selection criteria are applied to each jet to remove jets potentially dominated by instrumental effects or reconstruction failures [73].

3.3 Event selection and classification

Photon candidates are subject to a preselection that imposes requirements on p_T, H/E, and shower shape, and that uses an electron veto to reject photon candidates geometrically matched to at least two hits in the pixel detector. The electron veto is reinforced by an additional requirement that no photon candidate be also reconstructed as an electron candidate, which can happen if the candidate is associated with a track containing a single hit in the first layer of the pixel detector [57].

This preselection is designed to be slightly more stringent than the trigger requirements. A photon identification BDT, trained with the TMVA package [75], combining lateral shower shape and isolation variables [57], the median energy density, the pseudorapidity, and the raw energy is used to separate prompt photons from nonprompt photons resulting mainly from neutral-meson decays [49, 50]. Each photon candidate must satisfy the preselection requirements as well as a requirement on the minimum value of the photon identification BDT output score. The efficiencies of the minimum photon identification BDT output score requirement and preselection criteria (except for the electron veto requirements) are measured with a tag-and-probe technique applied to $Z \to e^+e^-$ events. The fractions of photons that satisfy the two electron-veto requirements are measured with $Z \to \mu^+\mu^-\gamma$ events, in which the photon is produced by final-state radiation providing a sample of prompt photons with purity higher than 99%. The ratios of the efficiencies in data and simulation are used to correct the signal efficiency in simulated signal samples and the associated statistical and systematic uncertainties are propagated to the expected signal yields.

The analysis uses all events that contain a diphoton pair where each of the photons in the pair satisfy a requirement on its p_T value as well as on the ratio of its p_T value to the invariant mass of the diphoton system, $m_{\gamma\gamma}$, that must lie within the range $65 < m_{\gamma\gamma} < 120\,\text{GeV}$. Specifically, the requirements are $p_T^{\gamma 1} > 30\,\text{GeV}$, $p_T^{\gamma 1}/m_{\gamma\gamma} > 0.47$ and $p_T^{\gamma 2} > 18\,\text{GeV}$, $p_T^{\gamma 2}/m_{\gamma\gamma} > 0.28$. Here, $\gamma 1$ ($\gamma 2$) refers to the photon candidate in the pair with the higher (lower) p_T value. The use of p_T thresholds scaled by $m_{\gamma\gamma}$ is intended to prevent a distortion of the low end of the diphoton mass spectrum that results if a fixed threshold is used [49, 50]; in particular, the minimum p_T values in the above fractions, 30.6 and 18.2 GeV, are chosen to be slightly higher than those of the HLT paths, i.e., 30 and 18 GeV, to further guard against distortion of the spectrum. To further discriminate against surviving electron pairs from DY events, we require that the natural logarithm of the sum of the squares of transverse momenta of all tracks associated with the chosen diphoton vertex, $\ln(\Sigma p_T^2/\,\text{GeV}^2)$, satisfy the requirement $\ln(\Sigma p_T^2/\,\text{GeV}^2) < 0.016 p_T^{\gamma\gamma}/\,\text{GeV} + 6.0$, where $p_T^{\gamma\gamma}$ is the transverse momentum of the selected diphoton candidate in each event. This requirement, optimized on surviving simulated DY and signal events, acts against tracks from DY electrons, the squared p_T of which are included in this sum, while preserving the efficiency of signal events, in particular those where the diphoton system is boosted. The efficiencies of this requirement in data and simulation are measured with $Z \to e^+e^-$ events, where the tracks matched to each of the two photon candidates have been removed. As with the preselection requirements, the data/simulation efficiency ratio is used to correct the signal sample efficiency, and the associated uncertainties are likewise propagated to the expected signal yields.

A multivariate event classifier [49, 50], the diphoton BDT, is used to discriminate between diphoton events from Higgs boson decays and those from the diphoton continuum, to further reduce background from events containing jets misidentified as isolated photons, and to assign higher scores to events with good diphoton mass resolution. Trained with the TMVA package, it incorporates the kinematic properties of the diphoton system (excluding $m_{\gamma\gamma}$), a per-event estimate of the diphoton mass resolution, and the photon identification BDT output values.

To target events produced via the VBF process, which feature two jets in the final state separated by a large rapidity gap, an additional multivariate discriminant [49, 50] is trained with the SCIKIT-LEARN package [76], for the analysis of the 2017 and 2018 data, to identify the distinctive kinematics of these jets, considering the ggH + jets production process as background. This discriminant is given as input to an additional multivariate classifier trained with SCIKIT-LEARN [49, 50], the combined BDT, along with the score from the diphoton BDT, and the ratio of the p_T of the diphoton system to its invariant mass, $p_T^{\gamma\gamma}/m_{\gamma\gamma}$.

As the first step of the classification process, events from the 2017 and 2018 data sets having two jets identified as not being compatible with pileup [50], satisfying the requirements $p_T^{j_1}(p_T^{j_2}) > 30\,(20)\,\text{GeV}$, $|\eta_{j_1(j_2)}| < 4.7$, where j_1 (j_2) refers to the jet with the highest (next-highest) p_T value, $m_{j_1 j_2} > 100\,\text{GeV}$, and having a minimum combined BDT classifier score value, are assigned to a "VBF class". The remaining events, as well as all those from the 2016 data set, are separated into classes based on the diphoton BDT score, with a minimum score below which they are rejected. The number of these classes and their boundaries are determined so as to maximize the expected signal significance for $m_H = 90\,\text{GeV}$, the midpoint of our search range, while providing a sufficient number of simulated events from Z boson dielectron decays for background modeling; different boundaries are used for the analysis of the 2016 data than for that of 2017 and 2018. Three such classes are used; they are referred to as 0, 1, 2, where class 0 contains the events with greatest expected sensitivity. The fraction of events containing more

than one diphoton candidate is of order 10^{-4}. In these cases, the candidate assigned to the highest sensitivity class is selected; should this class still contain multiple diphoton candidates, the candidate with the highest value of $p_{\mathrm{T}}^{\gamma 1} + p_{\mathrm{T}}^{\gamma 2}$ is then selected.

4 Signal parametrization

In order to perform a statistical interpretation of the data, it is necessary to have a description of the signal that includes the overall product of the efficiency and acceptance, as well as the shape of the diphoton mass distribution in each of the event classes. The simulated SM-like Higgs boson events are used to construct a parametrized signal model that is defined continuously for any value of the Higgs boson mass between 70 and 110 GeV. The photon energy resolution predicted by the simulation is modified by a Gaussian smearing determined from the comparison between the $\mathrm{Z} \to \mathrm{e}^+\mathrm{e}^-$ line-shape in data and simulation, where the electron energies have been corrected with factors developed for photons, using the same procedure as that described in Refs. [49, 50]. The amount of smearing is extracted differentially in bins of $|\eta|$ and the R_9 shower shape variable [52], defined as the energy sum of 3×3 crystals centered on the most energetic crystal in the ECAL cluster divided by the energy of the cluster. The trigger and preselection efficiency corrections described in Sections 3.1 and 3.3, respectively, are also applied to the simulated signal events.

Since the shape of the $m_{\gamma\gamma}$ distribution changes considerably depending on whether the vertex associated with the candidate diphoton is correctly identified, separate fits are made to the distributions for the correct and incorrect primary vertex selections when constructing the signal model. Events are considered to have the correct primary vertex if the z coordinate of the vertex associated with the candidate diphoton is within 1 cm in distance along the beam axis of the true vertex. For these events the signal shape is dominated by the ECAL response and reconstruction, and is modeled empirically with a sum of between two and four Gaussian functions depending on the data-taking period (2016, 2017, and 2018) and event class. The signal shape for events with an incorrect primary vertex selection is broadened significantly by the difference between the z coordinate position of the selected primary vertex and that of the true Higgs boson production vertex. The signal shape for these events is modeled with a sum of up to three Gaussian functions, depending on the data-taking period and event class. In both the correct and incorrect vertex assignment cases, the number of Gaussian functions is determined using an F-test [77], and the means, widths, and relative fractions of the Gaussian functions are extracted from the fits. For each production process, event class, and primary vertex identification correctness scenario, a simultaneous fit of signal samples [50] at m_{H} values in the range from 70 to 110 GeV is performed to obtain parametric variations with m_{H}, described by polynomials, of the Gaussian function parameters. The final fit function for each event class in each production process and each year is obtained by summing the individual functions for the two vertex scenarios. The relative size of the shapes associated with the two vertex scenarios, in each final function, is determined by the vertex selection efficiency.

The final parametrized shapes for the combination of all production mechanisms, for all event classes, weighted by their SM cross sections are shown in Fig. 1 for a Higgs boson mass of 90 GeV for the 2016, 2017, and 2018 data. Also shown are the full width at half maximum (FWHM) value and the value of the effective standard deviation (σ_{eff}), which is defined as half the width of the narrowest interval containing 68.3% of the invariant mass distribution. The product of efficiency and acceptance of the signal model ranges from 17.5 (16.0 and 16.9)% for $m_{\mathrm{H}} = 70$ GeV to 20.8 (19.9 and 20.8)% for $m_{\mathrm{H}} = 110$ GeV in the case of the 2016 (2017 and 2018) data.

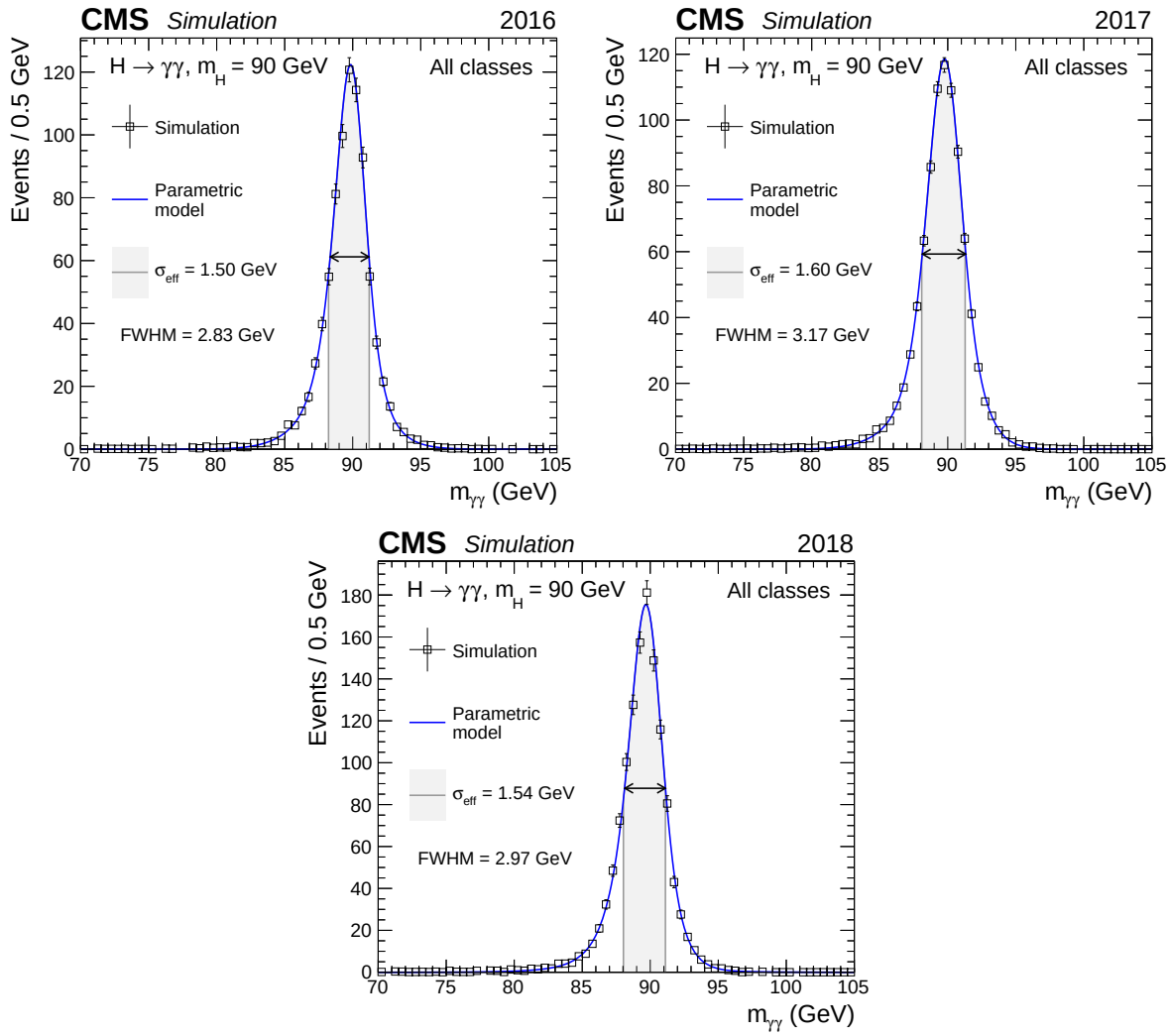

Figure 1: Full parametrized signal shape, integrated over all event classes, in simulated signal events with $m_{\mathrm{H}} = 90\,\mathrm{GeV}$ for 2016 (upper left), 2017 (upper right), and 2018 (lower). The open points are the weighted MC events and the blue lines the corresponding parametric models. Also shown are the σ_{eff} values and the shaded region limited by $\pm\sigma_{\mathrm{eff}}$, along with the FWHM values, indicated by the position of the arrows on each distribution.

5 Background estimation

In this analysis, as in Refs. [11, 49, 50], the background is modeled by fitting analytic functions to the observed diphoton mass distributions in each of the event classes. The fits are performed over the range $65 < m_{\gamma\gamma} < 120\,\mathrm{GeV}$. The model is determined from data with the discrete profiling method [78], which treats the choice of the background function as a discrete parameter in the likelihood fit to the data and estimates the systematic uncertainty associated with the choice of a particular function.

Since the search mass range of this analysis includes the Z boson peak region, a significant potential background source is DY dielectron production that, through misidentification, could appear as two isolated photons. An explicit component intended to describe the background from the DY process, in which the two apparently isolated photons survive all the selection requirements stated in Section 3.3, is added to the smoothly falling function [11, 49, 50] used to model the background. An exception is made for the events of the VBF class, where the

requirement on the minimum value of the combined BDT classifier is not imposed in order to obtain a sufficient number of events for the modeling. This additional component, referred to as "doubly-misidentified" events, is modeled with a double-sided Crystal Ball (DCB) function, which is a modification of the Crystal Ball function [79, 80] with an exponential tail on both sides, summed with an additional exponential function (DCB + exponential). The DCB function is characterized by seven parameters, including the number of events for normalization, and six shape parameters: the Gaussian mean and standard deviation, α_{L}, n_{L}, α_{R}, and n_{R}, where $\alpha_{\mathrm{L,R}}$ and $n_{\mathrm{L,R}}$ refer, respectively, to the slope and normalization of the left-hand (L) and right-hand (R) exponential tails. The additional exponential function contributes two supplementary parameters: p, the coefficient of the exponential argument and g, the fraction that the exponential function represents in the total DY process model. The values of these two parameters as well as those describing the DCB shape are determined by fitting the diphoton invariant mass distribution in a sample of simulated doubly-misidentified DY events for each event class. Because of the small size of the simulated event sample, we fix two of the six DCB shape parameters, α_{L} and α_{R}, to make the fit more stable. The fixed values are different in each event class and are obtained from fits of events where one photon candidate survives all selection requirements including the electron vetoes, and the other survives all selection requirements but fails the electron vetoes ("singly-misidentified" events). In each class, the value of the mean, which coincides with the peak position, lies somewhat below the nominal Z boson mass value. This bias is due to the fact that the electrons surviving the photon selection requirements (in particular the electron veto) have in general been poorly reconstructed, for example having undergone wide-angle bremsstrahlung of high-energy photons; furthermore, the electron energies have been corrected with factors developed for photons.

For the application of the discrete profiling method, members of several families of analytic functions, including exponential, power law, polynomials in the Bernstein basis, and Laurent series, are considered, each summed with the DCB + exponential function. The maximum order term in each series is determined using an F-test [77], and the minimum order, using a goodness-of-fit test. When fitting these functions to the $m_{\gamma\gamma}$ distribution in the data, the value of twice the negative logarithm of the likelihood (2NLL) is minimized. A penalty is added to the 2NLL value to take into account the number of floating parameters, including the fraction f of background events attributed to the component arising from the doubly-misidentified events (DCB + exponential fraction), in each candidate function.

The normalization of the DY background is determined from the fit. The shape parameters are fixed to the constant values that are obtained by fitting the doubly-misidentified DY events, as described above. In particular, the value of the Gaussian standard deviation in each event class for these doubly-misidentified events is greater than the corresponding value of σ_{eff} in the signal model by a factor of up to 2.

Table 1 shows, for each event class in each data-taking year, the functional family and order of the function chosen by the 2NLL minimization as being the best fit when summed with the DCB + exponential function, in the case of a background-only fit. Also shown are the DCB + exponential fractions for these chosen models in the subset of the diphoton mass range extending from 85 to 95 GeV, the mass range where the expected dielectron background from DY processes is most significant. These fractions range from 0.5 to 4.8% across the different years and event classes.

Binned likelihood fits of the chosen background models to the observed $m_{\gamma\gamma}$ distributions are performed, using 1 GeV bins and assuming no signal, and are shown for all the event classes in Figs. 2, 3, and 4 for the 2016, 2017, and 2018 data, respectively. The one- and two-standard

Table 1: Families and orders of functions chosen as best fit when summed with the DCB + exponential function, by year and by event class, in the case of background-only fits. The DCB + exponential fractions for these models in the range $85 < m_{\gamma\gamma} < 95\,\text{GeV}$ are also shown.

Event class		0	1	2	VBF
2016	Family/Order	Power Law 1	Bernstein 4	Exponential 3	—
	DCB + Exp. Fraction (%)	3.0	3.1	3.3	—
2017	Family/Order	Bernstein 3	Exponential 3	Bernstein 4	Bernstein 3
	DCB + Exp. Fraction (%)	2.7	1.4	1.9	2.6
2018	Family/Order	Laurent 1	Bernstein 4	Exponential 3	Bernstein 2
	DCB + Exp. Fraction (%)	0.5	4.1	4.8	0.8

deviation (σ) bands include only the uncertainty in the background model normalization associated with the statistical uncertainties of the fits, and are thus shown for illustration purposes only. These bands are obtained using an extended likelihood fit parametrized in terms of the background yield in bins corresponding to those used in Figs. 2, 3, and 4. The corresponding signal model for $m_{\mathrm{H}} = 90\,\text{GeV}$, multiplied by 10, is also shown for illustration purposes.

6 Systematic uncertainties

Many of the systematic uncertainties relevant to the analyses performed in Refs. [11, 49, 50] also apply to this analysis and are described briefly below. Additional uncertainties specific to this analysis are described in more detail.

6.1 Uncertainties evaluated at the per-photon level

The systematic uncertainties in the shape of the photon identification BDT distribution and in the per-photon energy resolution described in Refs. [49, 50] are applied in this analysis. These uncertainties propagate to the multivariate event classifier value, giving rise to the migration of events from one class to another, and to variations in the per-event efficiency in each class and for each production process. The uncertainties are evaluated using a signal sample with $m_{\mathrm{H}} = 90\,\text{GeV}$, the midpoint of the search range considered. For the 2016 data, the largest variation in efficiency due to the photon identification BDT distribution shape is 6.9%, for the $\mathrm{t\bar{t}H}$ process in event class 2; for the 2017 data, 6.4%, for the ggH process in event class 1, and for the 2018 data, 4.1% for the VBF process, also in event class 1. Otherwise, the variations are below 2.2/5.3/3.7% for the 2016/2017/2018 data sets. The largest variation in the efficiency due to the per-photon energy resolution applicable to the 2016 data is 18.2% for the ggH process in event class 1; for the 2017 data, 14.6% for the ggH process in class 1, and for the 2018 data, 13.7% for the $\mathrm{t\bar{t}H}$ process in class 2; otherwise the variations are below 12.9/13.7/11.9% for the 2016/2017/2018 data sets.

For the 2016/2017/2018 data, uncertainties in the trigger efficiencies give rise to efficiency variations of less than 0.8/1.8/0.5%. Uncertainties in the scale factors of the preselection give rise to efficiency variations of less than 3.3/3.2/5.2% in the case of the 2016/2017/2018 data. The uncertainties in the scale factors of the electron veto, of the requirement that a photon candidate may not be reconstructed as an electron, and of the minimum value of the photon identification BDT all contribute efficiency variations of less than 1% for the data of all three years.

The uncertainties in the measurement and in the correction of the photon energy scale in data, and in the correction of the energy resolution in simulation, arising from the methodology exploiting $\mathrm{Z} \to \mathrm{e^+e^-}$ events as described in Section 4 and Refs. [49, 50], are calculated in the same

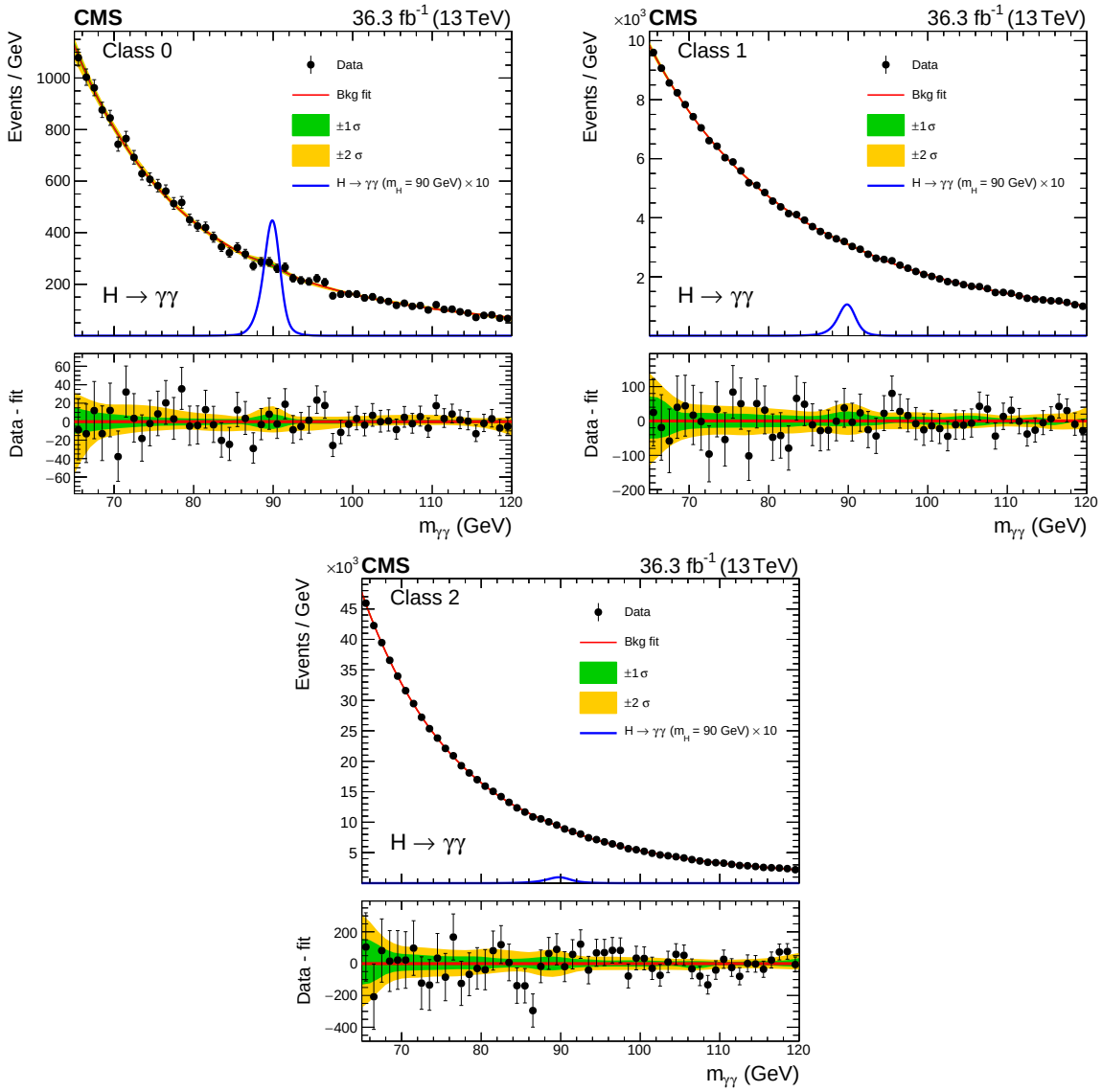

Figure 2: Background model fits using the chosen background model parametrization to the 2016 data in the three event classes. The corresponding signal model for each class and $m_{\mathrm{H}} = 90\,\mathrm{GeV}$, multiplied by 10, is also shown. The one- and two-σ bands reflect the uncertainty in the background model normalization associated with the statistical uncertainties of the fits, and are shown for illustration purposes only. The difference between the data and the background model is shown in the lower panels.

bins as the corrections themselves. Uncertainties arising from modeling of the material budget and of nonuniformity of light collection (the fraction of crystal scintillation light detected as a function of its longitudinal depth when emitted), nonlinearity in the photon energy scale between data and simulation, imperfect electromagnetic shower simulation, and vertex finding [49, 50], are propagated to the parametric signal model, where they result in uncertainties in the diphoton efficiency, mass scale, and resolution.

6.2 Uncertainties evaluated at the per-event level

The per-event systematic uncertainty in the total integrated luminosity, estimated from data [81–83], contributes an uncertainty of 1.2/2.3/2.5% in the signal yield for the 2016/2017/2018 data.

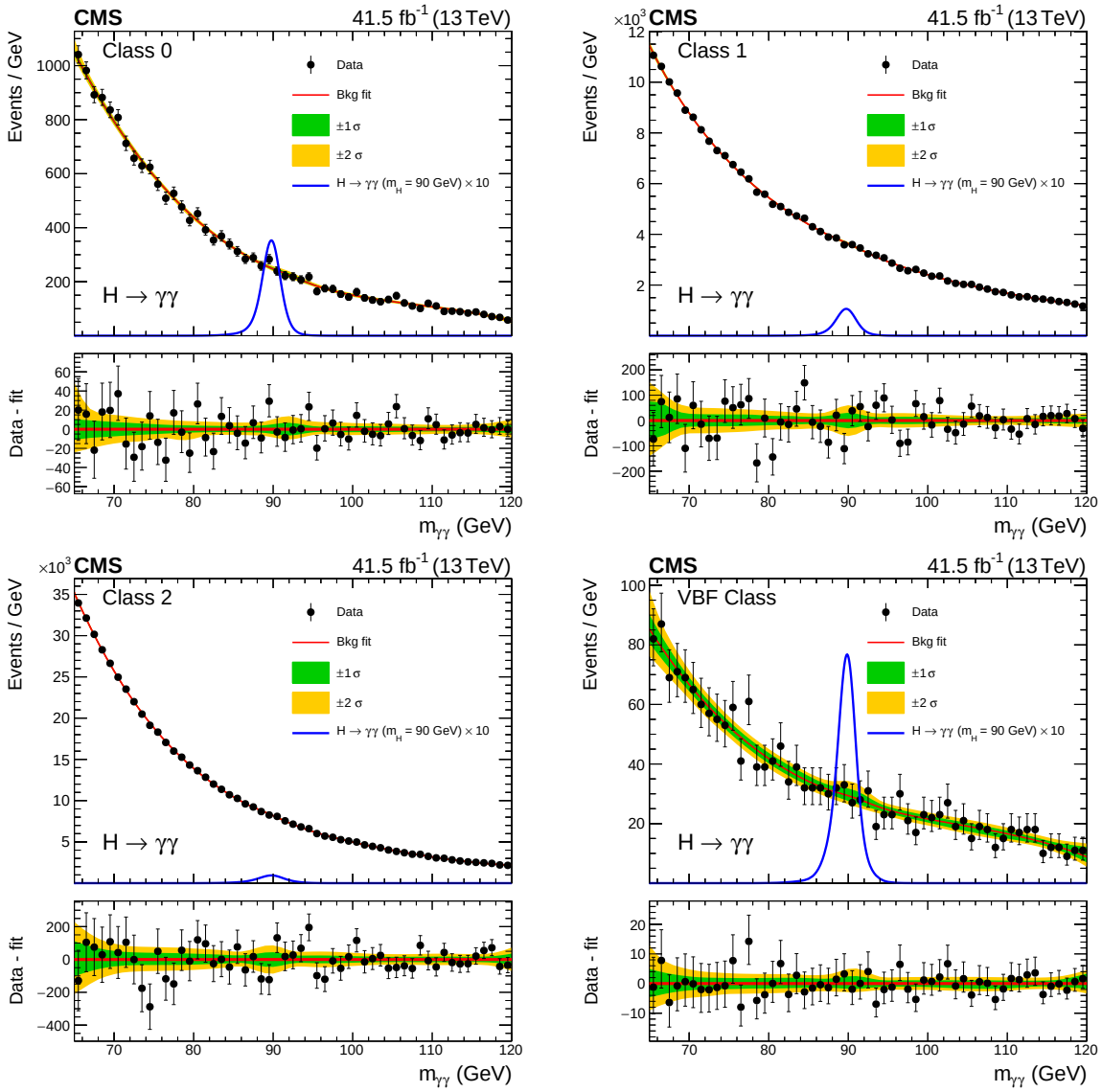

Figure 3: Background model fits using the chosen background model parametrization to the 2017 data in the four event classes. The corresponding signal model for each class and $m_{\mathrm{H}} = 90\,\mathrm{GeV}$, multiplied by 10, is also shown. The one- and two-σ bands reflect the uncertainty in the background model normalization associated with the statistical uncertainties of the fits, and are shown for illustration purposes only. The difference between the data and the background model is shown in the lower panels.

The overall uncertainty for the 2016–2018 period is 1.6%. The uncertainties for each data set are partially correlated to account for common sources in the luminosity measurement schemes.

For the analysis of the 2016 and 2017 data, an additional uncertainty in the signal efficiency is introduced to account for the gradual shift in the timing of the trigger inputs mentioned previously. It is largest for the VBF class in 2017, and amounts to less than 0.5 (1.9)% for 2016 (2017).

The systematic uncertainties from the theoretical predictions considered in this analysis are of three types. Firstly, the uncertainties in the signal acceptance due to changes in particle p_{T} and η values, arising from variations in the PDF and renormalization and factorization scales, are calculated [49, 50] using a signal sample with $m_{\mathrm{H}} = 90\,\mathrm{GeV}$. The NNPDF3.0 (NNPDF3.1)

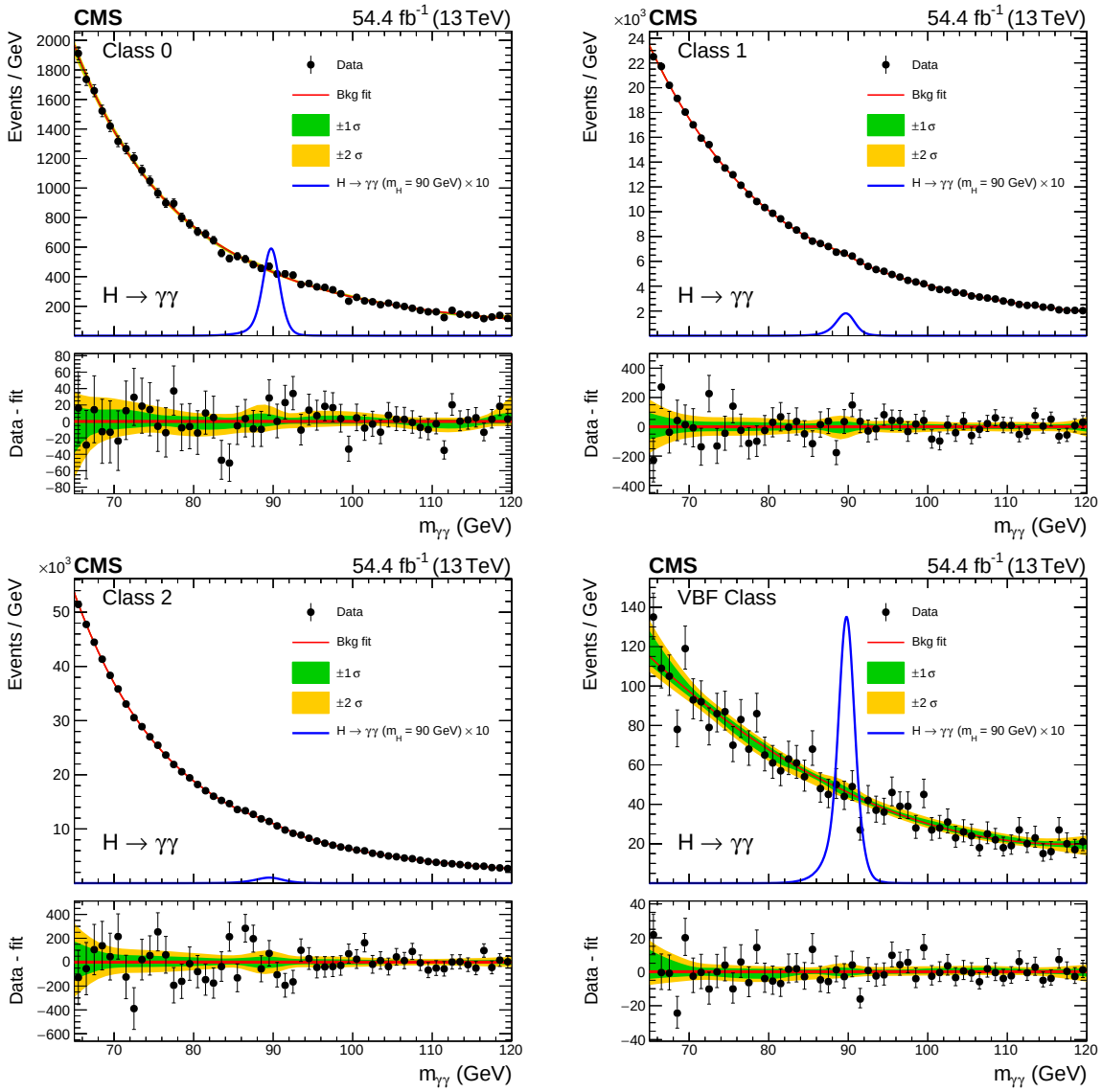

Figure 4: Background model fits using the chosen background model parametrization to the 2018 data in the four event classes. The corresponding signal model for each class and $m_{\mathrm{H}} = 90\,\mathrm{GeV}$, multiplied by 10, is also shown. The one- and two-σ bands reflect the uncertainty in the background model normalization associated with the statistical uncertainties of the fits, and are shown for illustration purposes only. The difference between the data and the background model is shown in the lower panels.

PDF set using the MC2HESSIAN procedure [84, 85] is used to estimate the PDF variations for 2016 (2017 and 2018). The effects due to variations of the strong coupling strength, α_{S}, are also considered, following the PDF4LHC prescription [67, 86]. The uncertainties due to PDF variations are negligible for all three data-taking years. The largest uncertainty due to scale variations in the 2016 (2017) data is 11.9 (10.0)% for the ggH production process in event class 0. In the 2018 data, the largest uncertainties also occur for the ggH process, with the maximum of 13.7% occurring in the VBF class. The uncertainties due to variations in α_{S} are largest for ggH production, in event class 0 at 1.9% for the 2016 data, and in the VBF class at 3.9 (4.1)% for the 2017 (2018) data; otherwise, they are below 0.5%.

Secondly, uncertainties in signal yields due to underlying event and parton shower modeling

are obtained using dedicated simulated samples for which the choice and specific tune of the event generator have been modified [87]. For the underlying event, these uncertainties are largest for the $t\bar{t}H$ production process in event class 2, amounting to 13.7% for 2016, and for the ZH production process in the VBF event class, amounting to 26.8 (20.4)% for 2017 (2018). In the case of the parton shower modeling, they are again largest for $t\bar{t}H$ production in event class 2 at 9.6% for the 2016 data, for ZH production in the VBF class at 15.9% for the 2017 data, and for the VBF production process in the VBF class at 12.0% for the 2018 data. Otherwise, they are typically below 7% for 2016 and 10% for 2017 and 2018.

Finally, the uncertainties in the production cross section for an SM-like Higgs boson, at a center-of-mass energy of 13 TeV, are accounted for by following the recommendations of the LHC Higgs cross section working group [67]. These uncertainties arise from uncertainties associated with particular choices of PDFs and QCD model parameters. They are used in the calculation of the expected and observed limits on the product of the production cross section and branching fraction into two photons relative to the expected value for an SM-like Higgs boson, and in the calculations of the expected and observed local p-values. The uncertainty in the branching fraction into two photons is neglected.

Uncertainties in the scale factor of the requirement on $\ln(\Sigma p_{\mathrm{T}}^2 / \mathrm{GeV}^2)$ give rise to efficiency variations of 0.4/0.9/0.5% in the case of the 2016/2017/2018 data.

For the analysis of the 2017 and 2018 data sets, changes in the presence or properties of jets affect the classification of events, potentially causing them to migrate between the VBF class and the other classes. Jet energy scale corrections account for a maximum uncertainty in signal yields of 14.9% (2017) and 15.8% (2018) in the VBF class. For the 2018 data, an additional uncertainty in jet energy scale is applied in order to cover a potential bias in the choice of the leading jets, stemming from a temporary readout interruption of the HCAL region extending between $-3.0 < \eta < -1.3$ and $-1.57 < \phi < 0.87$. This uncertainty is greatest for the VBF event class, ranging between 1 and 3% with a maximum of 3.4% for the ggH production process. For the other classes, it is in general less than 0.5%, reaching a maximum of 1.2% for the VBF production process in event class 0. For the VBF production process, another specific uncertainty in signal event yield arising from the implementation of the matching between matrix element and parton showers in the MC simulation, affecting jet kinematics, is applied; it ranges from 0.1 to 3% depending on the event class, reaching a maximum of 2.9 (2.6)% for the 2017 (2018) data in the VBF event class. The jet energy resolution contributes a signal yield uncertainty of less than 1.1% in 2017 and 3.0% in 2018. Finally, an uncertainty in signal yield due to pileup jet identification is estimated by comparing in data and simulation the identification score of jets in events with a Z boson and one balanced jet, and amounts to less than 4.1% in 2017 and 3.2% in 2018.

An additional source of per-event systematic uncertainty specific to this analysis is the modeling of the Z boson resonance component of the background. As explained previously, the parameters of the DCB function used to model the Z boson resonance are obtained from doubly-misidentified events, which are simulated DY events with all selection requirements applied including the electron veto requirements. These parameters could be different for data and simulation. To estimate these differences, we study simulated singly-misidentified events from the DY, diphoton, γ + jet, and QCD multijet processes. We fit the invariant diphoton mass of these events in data, in simulation including the sum of all background processes, and in simulated DY events alone, with a DCB + exponential component that describes the additional continuum background inherent in singly-misidentified events. We consider the pairwise differences among the DCB mean and standard deviation parameters extracted from these three

types of fits for each event class. The differences are considered statistically significant if they are greater than the quadratic sum of the statistical uncertainties from the fit. These differences contribute to the total systematic uncertainty in the DCB parameter values. The nominal parameter values are obtained from doubly-misidentified events so the differences contributing to the parameter uncertainties that are estimated from singly-misidentified events are doubled, to reflect the more conservative case where the parameters of the two photon candidates in a doubly-misidentified event are completely correlated.

The total systematic uncertainty in each event class for the mean and standard deviation parameters is the quadratic sum of: the statistical uncertainty from the fit to the doubly-misidentified simulated DY events; the doubled difference between the parameter values from data and from the sum of all simulated background processes, and the doubled difference between the parameter values from the sum of all simulated background processes and from simulated DY events alone, determined from the singly-misidentified events. In the case of the VBF class, an additional term, the doubled difference between the parameter values from simulated singly-misidentified DY events with and without the requirement on the minimum value of the combined BDT classifier, is added in the quadratic sum.

An uncertainty is assigned to the fixed values of the DCB parameters α_{L} and α_{R} for each event class by performing the fits of the doubly-misidentified simulated $\mathrm{Z} \to \mathrm{e}^{+}\mathrm{e}^{-}$ events with these two parameters allowed to float. The uncertainty is the quadratic sum of the statistical uncertainty in the fitted values of α_{L} and α_{R}, and the systematic uncertainty, which is taken as the difference between the fixed and fitted values for each of the two parameters.

Finally, the analysis takes into account the statistical uncertainties in the values of the DCB n_{L} and n_{R} parameters, and in the values of the additional exponential function p and g parameters, obtained from the fits to the doubly-misidentified simulated $\mathrm{Z} \to \mathrm{e}^{+}\mathrm{e}^{-}$ events.

The invariant mass distribution of electron pairs from surviving DY events has a shape that is similar to that of photon pairs in signal, when m_{H} is close to the fitted peak of the doubly-misidentified events. The systematic uncertainty in the fraction, f, of background events attributed to the surviving DY component, has been adjusted to minimize the potential bias induced by that shape similarity, while at the same time yielding a negligible effect on the expected limits and expected significances.

7 Results

Table 2 shows the expected numbers of signal events corresponding to the production of a hypothetical additional SM-like Higgs boson with $m_{\mathrm{H}} = 90\,\mathrm{GeV}$, from the analyses of the 2016, 2017, and 2018 data. The total number is broken down into the contributions from all the production processes in each of the event classes, where the VH processes (WH and ZH) are listed separately. Also shown are the σ_{eff} and σ_{HM} (defined as the FWHM divided by 2.35) values, as well as the number of background events per GeV estimated from the background-only fit to the data, that includes the number, shown separately, from the DY process, in the corresponding σ_{eff} window centered on $m_{\mathrm{H}} = 90\,\mathrm{GeV}$, using the chosen background function.

A simultaneous binned maximum likelihood fit to the diphoton invariant mass distributions in all event classes and in all three data-taking years, with a step size of 0.1 GeV, is performed over the range $70 < m_{\gamma\gamma} < 110\,\mathrm{GeV}$. The upper limits on the product of the cross section σ_{H} and branching fraction $\mathcal{B}$ into two photons are set using the $\mathrm{CL_s}$ modified frequentist criterion [88–90]. This construction uses the profile-likelihood ratio as the test statistic [91] under

Table 2: The expected number of SM-like Higgs boson signal events ($m_{\mathrm{H}} = 90\,\mathrm{GeV}$) per event class and the corresponding percentage breakdown per production process, for the 2016, 2017, and 2018 data. The values of σ_{eff} and σ_{HM} are also shown, along with the number of background events ("Bkg.") per GeV estimated from the background-only fit to the data, that includes the number, shown separately, from the DY process ("DY Bkg."), in a σ_{eff} window centered on $m_{\mathrm{H}} = 90\,\mathrm{GeV}$.

Event classes		Expected SM-like Higgs boson signal yield ($m_{\mathrm{H}} = 90\,\mathrm{GeV}$)								Bkg.	DY Bkg.
		Total	ggH (%)	VBF (%)	WH (%)	ZH (%)	$\mathrm{t\bar{t}H}$ (%)	σ_{eff} (GeV)	σ_{HM} (GeV)	(GeV^{-1})	(GeV^{-1})
2016	0	130	71.9	15.6	6.2	3.6	2.6	1.12	1.00	271	12
$36.3\,\mathrm{fb}^{-1}$	1	304	87.4	6.6	3.6	2.1	0.3	1.25	1.07	3093	33
	2	407	94.7	2.5	1.7	1.0	0.1	1.87	1.51	9190	193
	Total	842	88.5	6.0	3.1	1.8	0.6	1.50	1.20	12 554	239
2017	0	104	73.4	11.6	7.5	4.3	3.2	1.27	1.13	248	7
$41.5\,\mathrm{fb}^{-1}$	1	347	88.5	5.6	3.5	2.1	0.3	1.40	1.24	3625	83
	2	413	94.4	2.6	1.9	1.1	0.1	1.91	1.64	8169	244
	VBF	26	45.6	51.8	1.0	0.5	1.0	1.33	1.15	29	1
	Total	890	88.2	6.2	3.1	1.8	0.6	1.60	1.35	12 071	338
2018	0	162	75.1	10.2	7.3	4.3	3.0	1.21	1.05	430	3
$54.4\,\mathrm{fb}^{-1}$	1	585	90.1	4.8	3.1	1.8	0.2	1.34	1.17	6445	378
	2	473	94.4	2.5	1.9	1.2	0.1	2.01	1.73	10 982	720
	VBF	38	45.4	51.9	1.1	0.6	1.0	1.21	1.03	46	1
	Total	1258	88.4	6.1	3.1	1.8	0.6	1.54	1.27	17 902	1104

the asymptotic approximation. All of the experimental systematic uncertainties, except those pertaining to the integrated luminosity as previously noted, are assumed to be uncorrelated among the different data sets, as are the theoretical uncertainties in the signal acceptance due to PDF variations. The theoretical uncertainties in the signal acceptance due to scale variations as well as in the production cross sections at the center-of-mass energy of 13 TeV for an additional SM-like Higgs boson are assumed to be fully correlated. Figure 5 shows the expected and observed 95% confidence level (CL) upper limits on the product of σ_{H} and $\mathcal{B}$ into two photons, as a function of the mass of an additional SM-like Higgs boson in the range $70 < m_{\gamma\gamma} < 110\,\mathrm{GeV}$, calculated with respect to the background-only hypothesis, from the statistical combination of the 2016, 2017, and 2018 data sets.

The minimum (maximum) observed upper limit on the product of the production cross section and branching fraction is approximately 15 (73) fb, corresponding to a mass hypothesis of 108.9 (95.4) GeV.

In addition, the expected and observed 95% CL upper limits for the production of an additional SM-like Higgs boson via the sum of the fermion-coupled ggH and $\mathrm{t\bar{t}H}$ processes are shown in Fig. 6, for the combined data set. The limits for production via the sum of the vector boson-coupled VBF and VH processes are also shown. The production processes, in each case, are combined assuming relative proportions as predicted by the SM. The same limits are shown under the assumption of 100% production via each of the VBF and VH processes.

Figure 7 shows the observed local p-values as a function of the mass of an additional SM-like Higgs boson, calculated with respect to the background-only hypothesis, from the analyses of the data from 2016, 2017, 2018, and their statistical combination. The 2016 data reanalyzed with the new detector calibration show an excess that has increased in local significance with respect

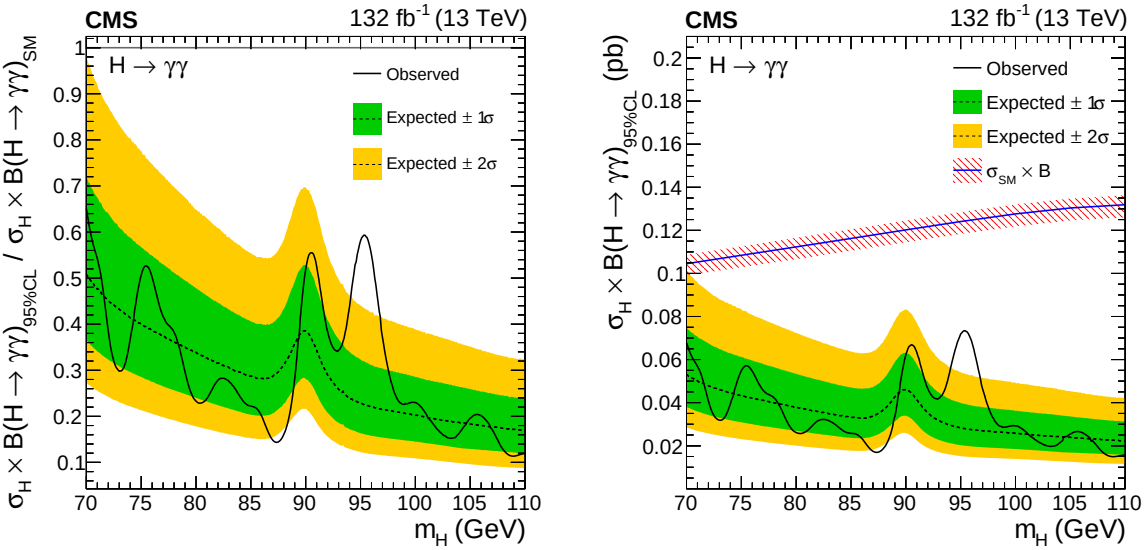

Figure 5: Expected and observed exclusion limits (95% CL, in the asymptotic approximation) on the product of the production cross section and branching fraction into two photons for an additional SM-like Higgs boson, from the statistical combination of the 2016, 2017, and 2018 data sets. The inner and outer bands indicate the regions containing the distribution of limits located within $\pm 1\sigma$ and $\pm 2\sigma$, respectively, of the expectation under the background-only hypothesis. The limit is shown relative to the expected SM-like value (left). The corresponding theoretical prediction for the product of the cross section and branching fraction into two photons for an additional SM-like Higgs boson is shown as a solid line with a hatched band, indicating its uncertainty [67] (right).

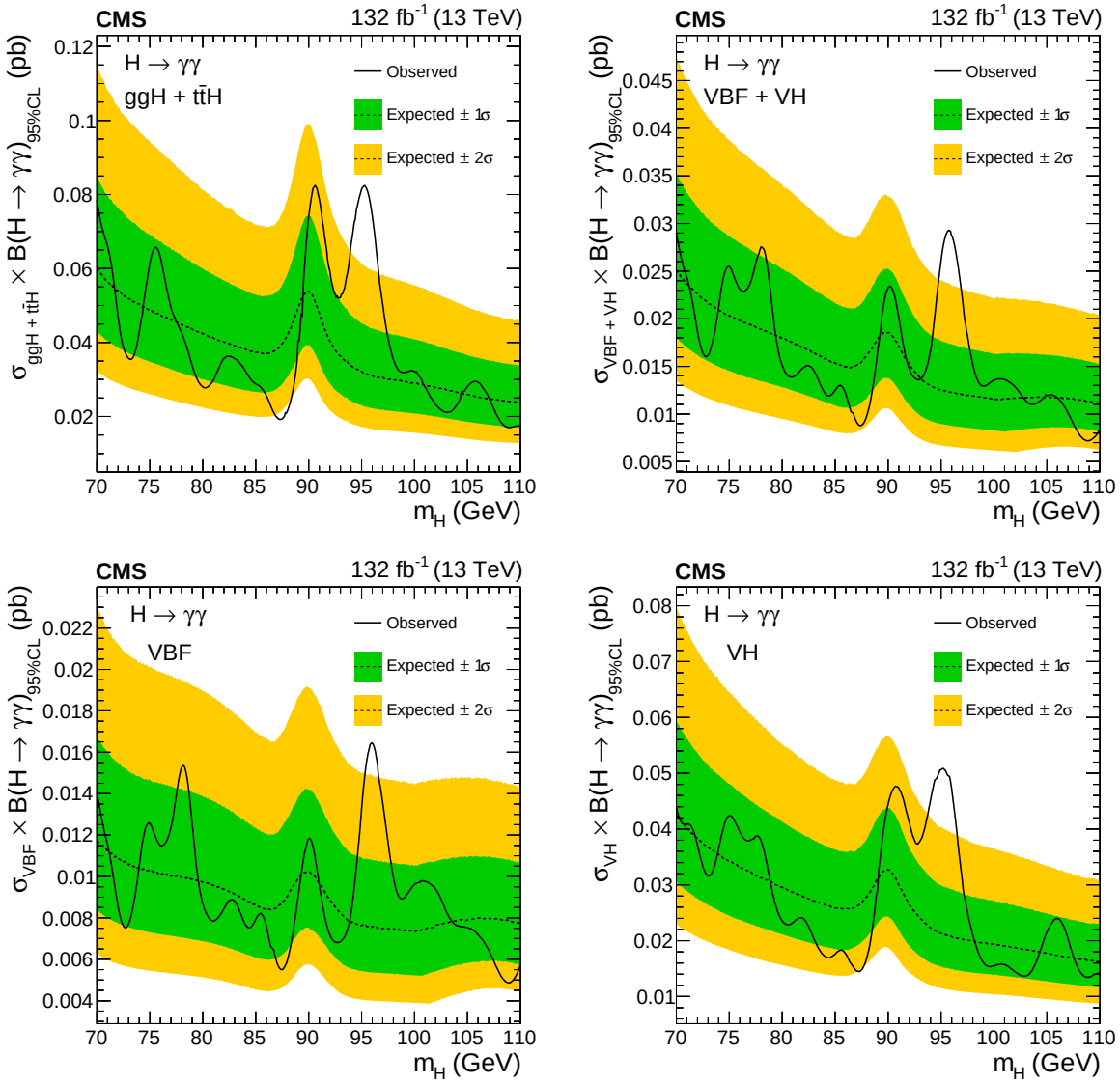

Figure 6: Expected and observed exclusion limits (95% CL, in the asymptotic approximation) on the product of the production cross section and branching fraction into two photons for an additional SM-like Higgs boson, for the ggH plus t$\bar{\text{t}}$H (upper left) and VBF plus VH (upper right) processes, and assuming 100% production via the VBF (lower left) or VH (lower right) processes, from the statistical combination of the 2016, 2017, and 2018 data sets. The inner and outer bands indicate the regions containing the distribution of limits located within $\pm 1\sigma$ and $\pm 2\sigma$, respectively, of the expectation under the background-only hypothesis.

to the previous analysis [47] from 2.8σ to 3.3σ at a mass of approximately 95.4 GeV. The local (global) significance decreases to 2.9σ (1.3σ) when the data from 2017 and 2018 are included. The global significance has been calculated using the method of Ref. [92].

8 Summary

A search for an additional, SM-like, low-mass Higgs boson decaying into two photons has been presented. It is based upon data samples corresponding to an integrated luminosity of 132 fb^{-1} collected in pp collisions at a center-of-mass energy of 13 TeV in 2016–2018. The search is per-

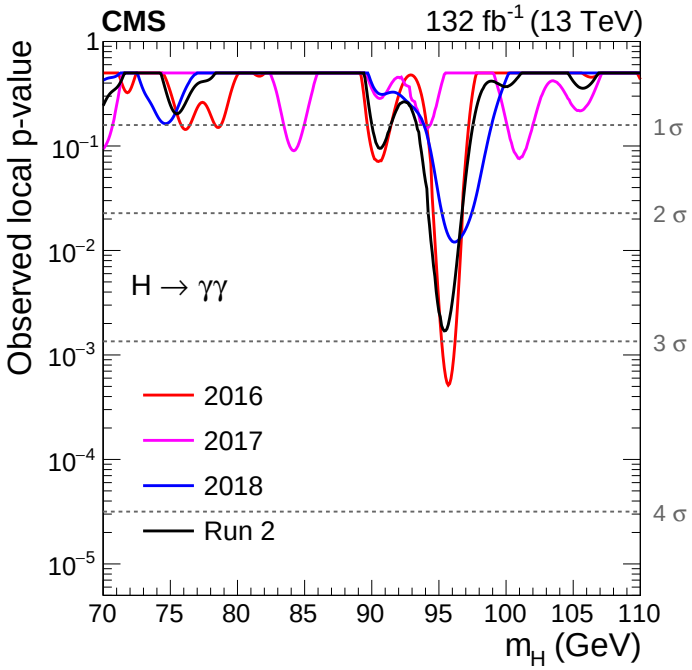

Figure 7: The observed local p-values for an additional SM-like Higgs boson as a function of m_{H}, from the analysis of the data from 2016, 2017, 2018, and their combination.

formed in a mass range between 70 and 110 GeV. The expected and observed 95% CL upper limits on the product of the production cross section and branching fraction into two photons for an additional SM-like Higgs boson as well as the expected and observed local p-values are presented. The observed upper limit on the product of the production cross section and branching fraction for the full data set ranges from 15 to 73 fb. The results of the statistical combination of the analyses of the three data sets show no significant excess over the background expectation. The maximum deviation with respect to the background is seen for a mass hypothesis of 95.4 GeV with a local (global) significance of 2.9 (1.3) standard deviations.

Acknowledgments

We congratulate our colleagues in the CERN accelerator departments for the excellent performance of the LHC and thank the technical and administrative staffs at CERN and at other CMS institutes for their contributions to the success of the CMS effort. In addition, we gratefully acknowledge the computing centers and personnel of the Worldwide LHC Computing Grid and other centers for delivering so effectively the computing infrastructure essential to our analyses. Finally, we acknowledge the enduring support for the construction and operation of the LHC, the CMS detector, and the supporting computing infrastructure provided by the following funding agencies: SC (Armenia), BMBWF and FWF (Austria); FNRS and FWO (Belgium); CNPq, CAPES, FAPERJ, FAPERGS, and FAPESP (Brazil); MES and BNSF (Bulgaria); CERN; CAS, MoST, and NSFC (China); MINCIENCIAS (Colombia); MSES and CSF (Croatia); RIF (Cyprus); SENESCYT (Ecuador); ERC PRG, RVTT3 and MoER TK202 (Estonia); Academy of Finland, MEC, and HIP (Finland); CEA and CNRS/IN2P3 (France); SRNSF (Georgia); BMBF, DFG, and HGF (Germany); GSRI (Greece); NKFIH (Hungary); DAE and DST (India); IPM (Iran); SFI (Ireland); INFN (Italy); MSIP and NRF (Republic of Korea); MES (Latvia); LMTLT (Lithuania); MOE and UM (Malaysia); BUAP, CINVESTAV, CONACYT, LNS, SEP, and

UASLP-FAI (Mexico); MOS (Montenegro); MBIE (New Zealand); PAEC (Pakistan); MES and NSC (Poland); FCT (Portugal); MESTD (Serbia); MCIN/AEI and PCTI (Spain); MOSTR (Sri Lanka); Swiss Funding Agencies (Switzerland); MST (Taipei); MHESI and NSTDA (Thailand); TUBITAK and TENMAK (Turkey); NASU (Ukraine); STFC (United Kingdom); DOE and NSF (USA).

Individuals have received support from the Indo-French Network in High Energy Physics financed by the Indo-French Center for the Promotion of Advanced Research (CEFIPRA/IFCPAR); the Marie-Curie program and the European Research Council and Horizon 2020 Grant, contract Nos. 675440, 724704, 752730, 758316, 765710, 824093, 101115353, 101002207, and COST Action CA16108 (European Union); the Leventis Foundation; the Alfred P. Sloan Foundation; the Alexander von Humboldt Foundation; the Science Committee, project no. 22rl-037 (Armenia); the Belgian Federal Science Policy Office; the Fonds pour la Formation à la Recherche dans l'Industrie et dans l'Agriculture (FRIA-Belgium); the Agentschap voor Innovatie door Wetenschap en Technologie (IWT-Belgium); the F.R.S.-FNRS and FWO (Belgium) under the "Excellence of Science – EOS" – be.h project n. 30820817; the Beijing Municipal Science & Technology Commission, No. Z191100007219010 and Fundamental Research Funds for the Central Universities (China); the Ministry of Education, Youth and Sports (MEYS) of the Czech Republic; the Shota Rustaveli National Science Foundation, grant FR-22-985 (Georgia); the Deutsche Forschungsgemeinschaft (DFG), under Germany's Excellence Strategy – EXC 2121 "Quantum Universe" – 390833306, and under project number 400140256 - GRK2497; the Hellenic Foundation for Research and Innovation (HFRI), Project Number 2288 (Greece); the Hungarian Academy of Sciences, the New National Excellence Program - ÚNKP, the NKFIH research grants K 131991, K 133046, K 138136, K 143460, K 143477, K 146913, K 146914, K 147048, 2020-2.2.1-ED-2021-00181, and TKP2021-NKTA-64 (Hungary); the Council of Science and Industrial Research, India; ICSC – National Research Center for High Performance Computing, Big Data and Quantum Computing and FAIR – Future Artificial Intelligence Research, funded by the NextGenerationEU program (Italy); the Latvian Council of Science; the Ministry of Education and Science, project no. 2022/WK/14, and the National Science Center, contracts Opus 2021/41/B/ST2/01369 and 2021/43/B/ST2/01552 (Poland); the Fundação para a Ciência e a Tecnologia, grant CEECIND/01334/2018 (Portugal); the National Priorities Research Program by Qatar National Research Fund; MCIN/AEI/10.13039/501100011033, ERDF "a way of making Europe", and the Programa Estatal de Fomento de la Investigación Científica y Técnica de Excelencia María de Maeztu, grant MDM-2017-0765 and Programa Severo Ochoa del Principado de Asturias (Spain); the Chulalongkorn Academic into Its 2nd Century Project Advancement Project, and the National Science, Research and Innovation Fund via the Program Management Unit for Human Resources & Institutional Development, Research and Innovation, grant B37G660013 (Thailand); the Kavli Foundation; the Nvidia Corporation; the SuperMicro Corporation; the Welch Foundation, contract C-1845; and the Weston Havens Foundation (USA).

References

[1] S. L. Glashow, "Partial-symmetries of weak interactions", *Nucl. Phys.* **22** (1961) 579, doi:10.1016/0029-5582(61)90469-2.

[2] S. Weinberg, "A model of leptons", *Phys. Rev. Lett.* **19** (1967) 1264, doi:10.1103/PhysRevLett.19.1264.

[3] A. Salam, "Weak and electromagnetic interactions", in *Elementary particle physics: relativistic groups and analyticity*, N. Svartholm, ed., p. 367. Almqvist & Wiksell, Stockholm, 1968. Proceedings of the eighth Nobel symposium.

[4] F. Englert and R. Brout, "Broken symmetry and the mass of gauge vector mesons", *Phys. Rev. Lett.* **13** (1964) 321, doi:10.1103/PhysRevLett.13.321.

[5] P. W. Higgs, "Broken symmetries, massless particles and gauge fields", *Phys. Lett.* **12** (1964) 132, doi:10.1016/0031-9163(64)91136-9.

[6] P. W. Higgs, "Broken symmetries and the masses of gauge bosons", *Phys. Rev. Lett.* **13** (1964) 508, doi:10.1103/PhysRevLett.13.508.

[7] G. S. Guralnik, C. R. Hagen, and T. W. B. Kibble, "Global conservation laws and massless particles", *Phys. Rev. Lett.* **13** (1964) 585, doi:10.1103/PhysRevLett.13.585.

[8] P. W. Higgs, "Spontaneous symmetry breakdown without massless bosons", *Phys. Rev.* **145** (1966) 1156, doi:10.1103/PhysRev.145.1156.

[9] T. W. B. Kibble, "Symmetry breaking in non-Abelian gauge theories", *Phys. Rev.* **155** (1967) 1554, doi:10.1103/PhysRev.155.1554.

[10] ATLAS Collaboration, "Observation of a new particle in the search for the standard model Higgs boson with the ATLAS detector at the LHC", *Phys. Lett. B* **716** (2012) 1, doi:10.1016/j.physletb.2012.08.020, arXiv:1207.7214.

[11] CMS Collaboration, "Observation of a new boson at a mass of 125 GeV with the CMS experiment at the LHC", *Phys. Lett. B* **716** (2012) 30, doi:10.1016/j.physletb.2012.08.021, arXiv:1207.7235.

[12] CMS Collaboration, "Observation of a new boson with mass near 125 GeV in pp collisions at $\sqrt{s}$ = 7 and 8 TeV", *JHEP* **06** (2013) 081, doi:10.1007/JHEP06(2013)081, arXiv:1303.4571.

[13] ATLAS Collaboration, "A detailed map of Higgs boson interactions by the ATLAS experiment ten years after the discovery", *Nature* **607** (2022) 52, doi:10.1038/s41586-022-04893-w, arXiv:2207.00092.

[14] CMS Collaboration, "A portrait of the Higgs boson by the CMS experiment ten years after the discovery", *Nature* **607** (2022) 60, doi:10.1038/s41586-022-04892-x, arXiv:2207.00043.

[15] A. Celis, V. Ilisie, and A. Pich, "LHC constraints on two-Higgs-doublet models", *JHEP* **07** (2013) 053, doi:10.1007/JHEP07(2013)053, arXiv:1302.4022.

[16] B. Coleppa, F. Kling, and S. Su, "Constraining type II 2HDM in light of LHC Higgs searches", *JHEP* **01** (2014) 161, doi:10.1007/JHEP01(2014)161, arXiv:1305.0002.

[17] S. Chang et al., "Two-Higgs-doublet models for the LHC Higgs boson data at $\sqrt{s} = 7$ and 8 TeV", *JHEP* **09** (2014) 101, doi:10.1007/JHEP09(2014)101, arXiv:1310.3374.

[18] J. Bernon et al., "Scrutinizing the alignment limit in two-Higgs-doublet models. II. $m_{\rm H} = 125\,\text{GeV}$", *Phys. Rev. D* **93** (2016) 035027, doi:10.1103/PhysRevD.93.035027, arXiv:1511.03682.

[19] G. Cacciapaglia et al., "Search for a lighter Higgs boson in two-Higgs-doublet models", *JHEP* **12** (2016) 68, doi:10.1007/JHEP12(2016)068, arXiv:1607.08653.

[20] P. Fayet, "Supergauge invariant extension of the Higgs mechanism and a model for the electron and its neutrino", *Nucl. Phys. B* **90** (1975) 104, doi:10.1016/0550-3213(75)90636-7.

[21] R. Barbieri, S. Ferrara, and C. A. Savoy, "Gauge models with spontaneously broken local supersymmetry", *Phys. Lett. B* **119** (1982) 343, doi:10.1016/0370-2693(82)90685-2.

[22] M. Dine, W. Fischler, and M. Srednicki, "A simple solution to the strong CP problem with a harmless axion", *Phys. Lett. B* **104** (1981) 199, doi:10.1016/0370-2693(81)90590-6.

[23] H. P. Nilles, M. Srednicki, and D. Wyler, "Weak interaction breakdown induced by supergravity", *Phys. Lett. B* **120** (1983) 346, doi:10.1016/0370-2693(83)90460-4.

[24] J. M. Frère, D. R. T. Jones, and S. Raby, "Fermion masses and induction of the weak scale by supergravity", *Nucl. Phys. B* **222** (1983) 11, doi:10.1016/0550-3213(83)90606-5.

[25] J. P. Derendinger and C. A. Savoy, "Quantum effects and SU(2) x U(1) breaking in supergravity gauge theories", *Nucl. Phys. B* **237** (1984) 307, doi:10.1016/0550-3213(84)90162-7.

[26] J. Ellis et al., "Higgs bosons in a nonminimal supersymmetric model", *Phys. Rev. D* **39** (1989) 844, doi:10.1103/PhysRevD.39.844.

[27] M. Drees, "Supersymmetric models with extended Higgs sector", *Int. J. Mod. Phys. A* **4** (1989) 3635, doi:10.1142/S0217751X89001448.

[28] U. Ellwanger, M. Rausch de Traubenberg, and C. A. Savoy, "Particle spectrum in supersymmetric models with a gauge singlet", *Phys. Lett. B* **315** (1993) 331, doi:10.1016/0370-2693(93)91621-S, arXiv:hep-ph/9307322.

[29] U. Ellwanger, M. Rausch de Traubenberg, and C. A. Savoy, "Higgs phenomenology of the supersymmetric model with a gauge singlet", *Z. Phys. C* **67** (1995) 665, doi:10.1007/BF01553993, arXiv:hep-ph/9502206.

[30] U. Ellwanger, M. Rausch de Traubenberg, and C. A. Savoy, "Phenomenology of supersymmetric models with a singlet", *Nucl. Phys. B* **492** (1997) 21, doi:10.1016/S0550-3213(97)00128-4, arXiv:hep-ph/9611251.

[31] T. Elliott, S. F. King, and P. L. White, "Unification constraints in the next-to-minimal supersymmetric standard model", *Phys. Lett. B* **351** (1995) 213, doi:10.1016/0370-2693(95)00381-T, arXiv:hep-ph/9406303.

[32] S. F. King and P. L. White, "Resolving the constrained minimal and next-to-minimal supersymmetric standard models", *Phys. Rev. D* **52** (1995) 4183, doi:10.1103/PhysRevD.52.4183, arXiv:hep-ph/9505326.

[33] F. Franke, "Neutralinos and Higgs bosons in the next-to-minimal supersymmetric standard model", *Int. J. Mod. Phys. A* **12** (1997) 479, doi:10.1142/S0217751X97000529, arXiv:hep-ph/9512366.

[34] M. Maniatis, "The next-to-minimal supersymmetric extension of the standard model reviewed", *Int. J. Mod. Phys. A* **25** (2010) 3505, doi:10.1142/S0217751X10049827, arXiv:0906.0777.

[35] U. Ellwanger, C. Hugonie, and A. M. Teixeira, "The next-to-minimal supersymmetric standard model", *Phys. Rept.* **496** (2010) 1, doi:10.1016/j.physrep.2010.07.001, arXiv:0910.1785.

[36] J.-W. Fan et al., "Study of diphoton decays of the lightest scalar Higgs boson in the next-to-minimal supersymmetric standard model", *Chin. Phys. C* **38** (2014) 073101, doi:10.1088/1674-1137/38/7/073101, arXiv:1309.6394.

[37] U. Ellwanger and M. Rodriguez-Vazquez, "Discovery prospects of a light scalar in the NMSSM", *JHEP* **02** (2016) 096, doi:10.1007/JHEP02(2016)096, arXiv:1512.04281.

[38] M. Guchait and J. Kumar, "Diphoton signal of light pseudoscalar in NMSSM at the LHC", *Phys. Rev. D* **95** (2017) 035036, doi:10.1103/PhysRevD.95.035036, arXiv:1608.05693.

[39] J. Cao et al., "Diphoton signal of the light Higgs boson in natural NMSSM", *Phys. Rev. D* **95** (2017) 116001, doi:10.1103/PhysRevD.95.116001, arXiv:1612.08522.

[40] J.-Q. Tao et al., "Search for a lighter Higgs boson in the next-to-minimal supersymmetric standard model", *Chin. Phys. C* **42** (2018) 103107, doi:10.1088/1674-1137/42/10/103107, arXiv:1805.11438.

[41] H. Georgi and M. Machacek, "Doubly-charged Higgs bosons", *Nucl. Phys. B* **262** (1985) 463, doi:10.1016/0550-3213(85)90325-6.

[42] H. E. Logan and V. Rentala, "All the generalized Georgi-Machacek models", *Phys. Rev. D* **92** (2015) 075011, doi:10.1103/PhysRevD.92.075011, arXiv:1502.01275.

[43] A. Ismail, B. Keeshan, H. E. Logan, and Y. Wu, "Benchmark for LHC searches for low-mass custodial fiveplet scalars in the Georgi-Machacek model", *Phys. Rev. D* **103** (2021) 095010, doi:10.1103/PhysRevD.103.095010, arXiv:2003.05536.

[44] C. Wang et al., "Search for a lighter neutral custodial fiveplet scalar in the Georgi-Machacek model", *Chin. Phys. C* **46** (2022) 083107, doi:10.1088/1674-1137/ac6cd3, arXiv:2204.09198.

[45] ALEPH Collaboration, DELPHI Collaboration, L3 Collaboration, OPAL Collaboration and the LEP working group for Higgs boson searches, "Search for the standard model Higgs boson at LEP", *Phys. Lett. B* **565** (2003) 61, doi:10.1016/S0370-2693(03)00614-2, arXiv:hep-ex/0306033.

[46] ATLAS Collaboration, "Search for scalar diphoton resonances in the mass range 65–600 GeV with the ATLAS detector in pp collision data at $\sqrt{s} = 8$ TeV", *Phys. Rev. Lett.* **113** (2014) 171801, doi:10.1103/PhysRevLett.113.171801, arXiv:1407.6583.

[47] CMS Collaboration, "Search for a standard model-like Higgs boson in the mass range between 70 and 110 GeV in the diphoton final state in proton-proton collisions at $\sqrt{s} = 8$ and 13 TeV", *Phys. Lett. B* **793** (2019) 320, doi:10.1016/j.physletb.2019.03.064, arXiv:1811.08459.

[48] HEPData record for this analysis, 2024. doi:10.17182/hepdata.150508.

[49] CMS Collaboration, "Observation of the diphoton decay of the Higgs boson and measurement of its properties", *Eur. Phys. J. C* **74** (2014) 3076, doi:10.1140/epjc/s10052-014-3076-z, arXiv:1407.0558.

[50] CMS Collaboration, "Measurements of Higgs boson properties in the diphoton decay channel in proton-proton collisions at $\sqrt{s} = 13$ TeV", *JHEP* **11** (2018) 185, doi:10.1007/JHEP11(2018)185, arXiv:1804.02716.

[51] CMS Collaboration, "The CMS experiment at the CERN LHC", *JINST* **3** (2008) S08004, doi:10.1088/1748-0221/3/08/S08004.

[52] CMS Collaboration, "Performance of photon reconstruction and identification with the CMS detector in proton-proton collisions at $\sqrt{s} = 8$ TeV", *JINST* **10** (2015) P08010, doi:10.1088/1748-0221/10/08/P08010, arXiv:1502.02702.

[53] CMS Collaboration, "A measurement of the Higgs boson mass in the diphoton decay channel", *Phys. Lett. B* **805** (2020) 135425, doi:10.1016/j.physletb.2020.135425, arXiv:2002.06398.

[54] CMS Collaboration, "Particle-flow reconstruction and global event description with the CMS detector", *JINST* **12** (2017) P10003, doi:10.1088/1748-0221/12/10/P10003, arXiv:1706.04965.

[55] CMS Collaboration, "Performance of the CMS Level-1 trigger in proton-proton collisions at $\sqrt{s} = 13$ TeV", *JINST* **15** (2020) P10017, doi:10.1088/1748-0221/15/10/P10017, arXiv:2006.10165.

[56] CMS Collaboration, "The CMS trigger system", *JINST* **12** (2017) P01020, doi:10.1088/1748-0221/12/01/P01020, arXiv:1609.02366.

[57] CMS Collaboration, "Electron and photon reconstruction and identification with the CMS experiment at the CERN LHC", *JINST* **16** (2021) P05014, doi:10.1088/1748-0221/16/05/P05014, arXiv:2012.06888.

[58] CMS Collaboration, "Measurement of the inclusive W and Z production cross sections in pp collisions at $\sqrt{s} = 7$ TeV", *JHEP* **10** (2011) 132, doi:10.1007/JHEP10(2011)132, arXiv:1107.4789.

[59] J. Alwall et al., "The automated computation of tree-level and next-to-leading order differential cross sections, and their matching to parton shower simulations", *JHEP* **07** (2014) 079, doi:10.1007/JHEP07(2014)079, arXiv:1405.0301.

[60] R. Frederix and S. Frixione, "Merging meets matching in MC@NLO", *JHEP* **12** (2012) 061, doi:10.1007/JHEP12(2012)061, arXiv:1209.6215.

[61] NNPDF Collaboration, "Parton distributions for the LHC run II", *JHEP* **04** (2015) 040, doi:10.1007/JHEP04(2015)040, arXiv:1410.8849.

[62] NNPDF Collaboration, "Parton distributions from high-precision collider data", *Eur. Phys. J. C* **77** (2017) 663, doi:10.1140/epjc/s10052-017-5199-5, arXiv:1706.00428.

[63] K. Hamilton, P. Nason, E. Re, and G. Zanderighi, "NNLOPS simulation of Higgs boson production", *JHEP* **10** (2013) 222, doi:10.1007/JHEP10(2013)222, arXiv:1309.0017.

[64] T. Sjöstrand et al., "An introduction to PYTHIA 8.2", *Comput. Phys. Commun.* **191** (2015) 159, doi:10.1016/j.cpc.2015.01.024, arXiv:1410.3012.

[65] CMS Collaboration, "Event generator tunes obtained from underlying event and multiparton scattering measurements", *Eur. Phys. J. C* **76** (2016) 155, doi:10.1140/epjc/s10052-016-3988-x, arXiv:1512.00815.

[66] CMS Collaboration, "Extraction and validation of a new set of CMS PYTHIA8 tunes from underlying-event measurements", *Eur. Phys. J. C* **80** (2020) 4, doi:10.1140/epjc/s10052-019-7499-4, arXiv:1903.12179.

[67] LHC Higgs Cross Section Working Group, "Handbook of LHC Higgs cross sections: 4. deciphering the nature of the Higgs sector", *CERN* (2016) doi:10.23731/CYRM-2017-002, arXiv:1610.07922.

[68] GEANT4 Collaboration, "GEANT4—a simulation toolkit", *Nucl. Instrum. Meth. A* **506** (2003) 250, doi:10.1016/S0168-9002(03)01368-8.

[69] T. Gleisberg et al., "Event generation with SHERPA 1.1", *JHEP* **02** (2009) 007, doi:10.1088/1126-6708/2009/02/007, arXiv:0811.4622.

[70] CMS Collaboration, "Energy calibration and resolution of the CMS electromagnetic calorimeter in pp collisions at $\sqrt{s} = 7$ TeV", *JINST* **8** (2013) P09009, doi:10.1088/1748-0221/8/09/P09009, arXiv:1306.2016.

[71] M. Cacciari, G. P. Salam, and G. Soyez, "The anti-k_T jet clustering algorithm", *JHEP* **04** (2008) 063, doi:10.1088/1126-6708/2008/04/063, arXiv:0802.1189.

[72] M. Cacciari, G. P. Salam, and G. Soyez, "FastJet user manual", *Eur. Phys. J. C* **72** (2012) 1896, doi:10.1140/epjc/s10052-012-1896-2, arXiv:1111.6097.

[73] CMS Collaboration, "Pileup mitigation at CMS in 13 TeV data", *JINST* **15** (2020) P09018, doi:10.1088/1748-0221/15/09/P09018, arXiv:2003.00503.

[74] CMS Collaboration, "Jet energy scale and resolution in the CMS experiment in pp collisions at 8 TeV", *JINST* **12** (2017) P02014, doi:10.1088/1748-0221/12/02/P02014, arXiv:1607.03663.

[75] A. Hoecker et al., "TMVA—toolkit for multivariate data analysis", 2007. arXiv:physics/0703039.

[76] F. Pedregosa et al., "Scikit-learn: machine learning in Python", *J. Machine Learning Res.* **12** (2011) 2825, doi:10.48550/arXiv.1201.0490, arXiv:1201.0490.

[77] R. A. Fisher, "On the interpretation of χ^2 from contingency tables, and the calculation of p", *J. Royal Stat. Soc* **85** (1922) 87, doi:10.2307/2340521.

[78] P. D. Dauncey, M. Kenzie, N. Wardle, and G. J. Davies, "Handling uncertainties in background shapes: the discrete profiling method", *JINST* **10** (2015) P04015, doi:10.1088/1748-0221/10/04/P04015, arXiv:1408.6865.

[79] M. Oreglia, "A study of the reactions $\psi' \to \gamma\gamma\psi$". PhD thesis, Stanford University, 1980. SLAC Report SLAC-R-236.

[80] T. Skwarnicki, "A study of the radiative CASCADE transitions between the Upsilon-prime and Upsilon resonances". PhD thesis, Cracow, INP, 1986.

[81] CMS Collaboration, "Precision luminosity measurement in proton-proton collisions at $\sqrt{s} = 13$ TeV in 2015 and 2016 at CMS", *Eur. Phys. J. C* **81** (2021) 800, doi:10.1140/epjc/s10052-021-09538-2, arXiv:2104.01927.

[82] CMS Collaboration, "CMS luminosity measurement for the 2017 data-taking period at $\sqrt{s} = 13$ TeV", CMS Physics Analysis Summary CMS-PAS-LUM-17-004, 2018.

[83] CMS Collaboration, "CMS luminosity measurement for the 2018 data-taking period at $\sqrt{s} = 13$ TeV", CMS Physics Analysis Summary CMS-PAS-LUM-18-002, 2019.

[84] S. Carrazza et al., "An unbiased Hessian representation for Monte Carlo PDFs", *Eur. Phys. J. C* **75** (2015) 369, doi:10.1140/epjc/s10052-015-3590-7, arXiv:1505.06736.

[85] J. Gao and P. Nadolsky, "A meta-analysis of parton distribution functions", *JHEP* **07** (2014) 035, doi:10.1007/jhep07(2014)035, arXiv:1401.0013.

[86] J. Butterworth et al., "PDF4LHC recommendations for LHC Run II", *J. Phys. G* **43** (2016) 023001, doi:10.1088/0954-3899/43/2/023001, arXiv:1510.03865.

[87] CMS Collaboration, "Measurements of Higgs boson production cross sections and couplings in the diphoton decay channel at $\sqrt{s} = 13$ TeV", *JHEP* **07** (2021) 027, doi:10.1007/jhep07(2021)027, arXiv:2103.06956.

[88] ATLAS and CMS Collaborations, LHC Higgs Combination Group, "Procedure for the LHC Higgs boson search combination in Summer 2011", CMS Note CMS-NOTE-2011-005, ATL-PHYS-PUB-2011-11, CERN, 2011.

[89] T. Junk, "Confidence level computation for combining searches with small statistics", *Nucl. Instrum. Meth. A* **434** (1999) 435, doi:10.1016/S0168-9002(99)00498-2, arXiv:hep-ex/9902006.

[90] A. L. Read, "Presentation of search results: the CL_s technique", *J. Phys. G* **28** (2002) 2693, doi:10.1088/0954-3899/28/10/313.

[91] G. Cowan, K. Cranmer, E. Gross, and O. Vitells, "Asymptotic formulae for likelihood-based tests of new physics", *Eur. Phys. J. C* **71** (2011) 1554, doi:10.1140/epjc/s10052-011-1554-0, arXiv:1007.1727. [Erratum: doi:10.1140/epjc/s10052-013-2501-z].

[92] L. Demortier, "P-values and nuisance parameters", in *Statistical issues for LHC physics. Proceedings, Workshop, PHYSTAT-LHC, Geneva, Switzerland, June 27-29, 2007*, p. 23. 2008. doi:10.5170/CERN-2008-001.

A The CMS Collaboration

Yerevan Physics Institute, Yerevan, Armenia
A. Hayrapetyan, A. Tumasyan[1]

Institut für Hochenergiephysik, Vienna, Austria
W. Adam, J.W. Andrejkovic, T. Bergauer, S. Chatterjee, K. Damanakis, M. Dragicevic, A. Escalante Del Valle, P.S. Hussain, M. Jeitler[2], N. Krammer, A. Li, D. Liko, I. Mikulec, J. Schieck[2], R. Schöfbeck, D. Schwarz, M. Sonawane, S. Templ, W. Waltenberger, C.-E. Wulz[2]

Universiteit Antwerpen, Antwerpen, Belgium
M.R. Darwish[3], T. Janssen, P. Van Mechelen

Vrije Universiteit Brussel, Brussel, Belgium
E.S. Bols, J. D'Hondt, S. Dansana, A. De Moor, M. Delcourt, H. El Faham, S. Lowette, I. Makarenko, D. Müller, A.R. Sahasransu, S. Tavernier, M. Tytgat[4], S. Van Putte, D. Vannerom

Université Libre de Bruxelles, Bruxelles, Belgium
B. Clerbaux, G. De Lentdecker, L. Favart, D. Hohov, J. Jaramillo, A. Khalilzadeh, K. Lee, M. Mahdavikhorrami, A. Malara, S. Paredes, L. Pétré, N. Postiau, L. Thomas, M. Vanden Bemden, C. Vander Velde, P. Vanlaer

Ghent University, Ghent, Belgium
M. De Coen, D. Dobur, Y. Hong, J. Knolle, L. Lambrecht, G. Mestdach, C. Rendón, A. Samalan, K. Skovpen, N. Van Den Bossche, L. Wezenbeek

Université Catholique de Louvain, Louvain-la-Neuve, Belgium
A. Benecke, G. Bruno, C. Caputo, C. Delaere, I.S. Donertas, A. Giammanco, K. Jaffel, Sa. Jain, V. Lemaitre, J. Lidrych, P. Mastrapasqua, K. Mondal, T.T. Tran, S. Wertz

Centro Brasileiro de Pesquisas Fisicas, Rio de Janeiro, Brazil
G.A. Alves, E. Coelho, C. Hensel, T. Menezes De Oliveira, A. Moraes, P. Rebello Teles, M. Soeiro

Universidade do Estado do Rio de Janeiro, Rio de Janeiro, Brazil
W.L. Aldá Júnior, M. Alves Gallo Pereira, M. Barroso Ferreira Filho, H. Brandao Malbouisson, W. Carvalho, J. Chinellato[5], E.M. Da Costa, G.G. Da Silveira[6], D. De Jesus Damiao, S. Fonseca De Souza, J. Martins[7], C. Mora Herrera, K. Mota Amarilo, L. Mundim, H. Nogima, A. Santoro, A. Sznajder, M. Thiel, A. Vilela Pereira

Universidade Estadual Paulista, Universidade Federal do ABC, São Paulo, Brazil
C.A. Bernardes[6], L. Calligaris, T.R. Fernandez Perez Tomei, E.M. Gregores, P.G. Mercadante, S.F. Novaes, B. Orzari, Sandra S. Padula

Institute for Nuclear Research and Nuclear Energy, Bulgarian Academy of Sciences, Sofia, Bulgaria
A. Aleksandrov, G. Antchev, R. Hadjiiska, P. Iaydjiev, M. Misheva, M. Shopova, G. Sultanov

University of Sofia, Sofia, Bulgaria
A. Dimitrov, L. Litov, B. Pavlov, P. Petkov, A. Petrov, E. Shumka

Instituto De Alta Investigación, Universidad de Tarapacá, Casilla 7 D, Arica, Chile
S. Keshri, S. Thakur

Beihang University, Beijing, China
T. Cheng, Q. Guo, T. Javaid, M. Mittal, L. Yuan

Department of Physics, Tsinghua University, Beijing, China
G. Bauer[8,9], Z. Hu, J. Liu, K. Yi[8,10]

Institute of High Energy Physics, Beijing, China
G.M. Chen[11], H.S. Chen[11], M. Chen[11], F. Iemmi, C.H. Jiang, A. Kapoor[12], H. Liao, Z.-A. Liu[13], F. Monti, M.A. Shahzad[11], R. Sharma[14], J.N. Song[13], J. Tao, C. Wang[11], J. Wang, Z. Wang[11], H. Zhang

State Key Laboratory of Nuclear Physics and Technology, Peking University, Beijing, China
A. Agapitos, Y. Ban, A. Levin, C. Li, Q. Li, Y. Mao, S.J. Qian, X. Sun, D. Wang, H. Yang, L. Zhang, C. Zhou

Sun Yat-Sen University, Guangzhou, China
Z. You

University of Science and Technology of China, Hefei, China
N. Lu

Institute of Modern Physics and Key Laboratory of Nuclear Physics and Ion-beam Application (MOE) - Fudan University, Shanghai, China
X. Gao[15], D. Leggat, H. Okawa, Y. Zhang

Zhejiang University, Hangzhou, Zhejiang, China
Z. Lin, C. Lu, M. Xiao

Universidad de Los Andes, Bogota, Colombia
C. Avila, D.A. Barbosa Trujillo, A. Cabrera, C. Florez, J. Fraga, J.A. Reyes Vega

Universidad de Antioquia, Medellin, Colombia
J. Mejia Guisao, F. Ramirez, M. Rodriguez, J.D. Ruiz Alvarez

University of Split, Faculty of Electrical Engineering, Mechanical Engineering and Naval Architecture, Split, Croatia
D. Giljanovic, N. Godinovic, D. Lelas, A. Sculac

University of Split, Faculty of Science, Split, Croatia
M. Kovac, T. Sculac[16]

Institute Rudjer Boskovic, Zagreb, Croatia
P. Bargassa, V. Brigljevic, B.K. Chitroda, D. Ferencek, S. Mishra, A. Starodumov[17], T. Susa

University of Cyprus, Nicosia, Cyprus
A. Attikis, K. Christoforou, S. Konstantinou, J. Mousa, C. Nicolaou, F. Ptochos, P.A. Razis, H. Rykaczewski, H. Saka, A. Stepennov

Charles University, Prague, Czech Republic
M. Finger, M. Finger Jr., A. Kveton

Escuela Politecnica Nacional, Quito, Ecuador
E. Ayala

Universidad San Francisco de Quito, Quito, Ecuador
E. Carrera Jarrin

Academy of Scientific Research and Technology of the Arab Republic of Egypt, Egyptian Network of High Energy Physics, Cairo, Egypt
Y. Assran[18,19], S. Elgammal[19]

Center for High Energy Physics (CHEP-FU), Fayoum University, El-Fayoum, Egypt
A. Lotfy, M.A. Mahmoud

National Institute of Chemical Physics and Biophysics, Tallinn, Estonia
R.K. Dewanjee[20], K. Ehataht, M. Kadastik, T. Lange, S. Nandan, C. Nielsen, J. Pata, M. Raidal, L. Tani, C. Veelken

Department of Physics, University of Helsinki, Helsinki, Finland
H. Kirschenmann, K. Osterberg, M. Voutilainen

Helsinki Institute of Physics, Helsinki, Finland
S. Bharthuar, E. Brücken, F. Garcia, J. Havukainen, K.T.S. Kallonen, R. Kinnunen, T. Lampén, K. Lassila-Perini, S. Lehti, T. Lindén, M. Lotti, L. Martikainen, M. Myllymäki, M.m. Rantanen, H. Siikonen, E. Tuominen, J. Tuominiemi

Lappeenranta-Lahti University of Technology, Lappeenranta, Finland
P. Luukka, H. Petrow, T. Tuuva[†]

IRFU, CEA, Université Paris-Saclay, Gif-sur-Yvette, France
M. Besancon, F. Couderc, M. Dejardin, D. Denegri, J.L. Faure, F. Ferri, S. Ganjour, P. Gras, G. Hamel de Monchenault, V. Lohezic, J. Malcles, J. Rander, A. Rosowsky, M.Ö. Sahin, A. Savoy-Navarro[21], P. Simkina, M. Titov, M. Tornago

Laboratoire Leprince-Ringuet, CNRS/IN2P3, Ecole Polytechnique, Institut Polytechnique de Paris, Palaiseau, France
C. Baldenegro Barrera, F. Beaudette, A. Buchot Perraguin, P. Busson, A. Cappati, C. Charlot, F. Damas, O. Davignon, A. De Wit, G. Falmagne, B.A. Fontana Santos Alves, S. Ghosh, A. Gilbert, R. Granier de Cassagnac, A. Hakimi, B. Harikrishnan, L. Kalipoliti, G. Liu, J. Motta, M. Nguyen, C. Ochando, L. Portales, R. Salerno, U. Sarkar, J.B. Sauvan, Y. Sirois, A. Tarabini, E. Vernazza, A. Zabi, A. Zghiche

Université de Strasbourg, CNRS, IPHC UMR 7178, Strasbourg, France
J.-L. Agram[22], J. Andrea, D. Apparu, D. Bloch, J.-M. Brom, E.C. Chabert, C. Collard, S. Falke, U. Goerlach, C. Grimault, R. Haeberle, A.-C. Le Bihan, G. Saha, M.A. Sessini, P. Van Hove

Institut de Physique des 2 Infinis de Lyon (IP2I), Villeurbanne, France
S. Beauceron, B. Blancon, G. Boudoul, N. Chanon, J. Choi, D. Contardo, P. Depasse, C. Dozen[23], H. El Mamouni, J. Fay, S. Gascon, M. Gouzevitch, C. Greenberg, G. Grenier, B. Ille, I.B. Laktineh, M. Lethuillier, L. Mirabito, S. Perries, A. Purohit, M. Vander Donckt, P. Verdier, J. Xiao

Georgian Technical University, Tbilisi, Georgia
D. Chokheli, I. Lomidze, Z. Tsamalaidze[17]

RWTH Aachen University, I. Physikalisches Institut, Aachen, Germany
V. Botta, L. Feld, K. Klein, M. Lipinski, D. Meuser, A. Pauls, N. Röwert,

M. Teroerde

RWTH Aachen University, III. Physikalisches Institut A, Aachen, Germany
S. Diekmann, A. Dodonova, N. Eich, D. Eliseev, F. Engelke, M. Erdmann, P. Fackeldey, B. Fischer, T. Hebbeker, K. Hoepfner, F. Ivone, A. Jung, M.y. Lee, L. Mastrolorenzo, M. Merschmeyer, A. Meyer, S. Mukherjee, D. Noll, A. Novak, F. Nowotny, A. Pozdnyakov, Y. Rath, W. Redjeb, F. Rehm, H. Reithler, V. Sarkisovi, A. Schmidt, A. Sharma, J.L. Spah, A. Stein, F. Torres Da Silva De Araujo[24], L. Vigilante, S. Wiedenbeck, S. Zaleski

RWTH Aachen University, III. Physikalisches Institut B, Aachen, Germany
C. Dziwok, G. Flügge, W. Haj Ahmad[25], T. Kress, A. Nowack, O. Pooth, A. Stahl, T. Ziemons, A. Zotz

Deutsches Elektronen-Synchrotron, Hamburg, Germany
H. Aarup Petersen, M. Aldaya Martin, J. Alimena, S. Amoroso, Y. An, S. Baxter, M. Bayatmakou, H. Becerril Gonzalez, O. Behnke, A. Belvedere, S. Bhattacharya, F. Blekman[26], K. Borras[27], D. Brunner, A. Campbell, A. Cardini, C. Cheng, F. Colombina, S. Consuegra Rodríguez, G. Correia Silva, M. De Silva, G. Eckerlin, D. Eckstein, L.I. Estevez Banos, O. Filatov, E. Gallo[26], A. Geiser, A. Giraldi, G. Greau, V. Guglielmi, M. Guthoff, A. Hinzmann, A. Jafari[28], L. Jeppe, N.Z. Jomhari, B. Kaech, M. Kasemann, H. Kaveh, C. Kleinwort, R. Kogler, M. Komm, D. Krücker, W. Lange, D. Leyva Pernia, K. Lipka[29], W. Lohmann[30], R. Mankel, I.-A. Melzer-Pellmann, M. Mendizabal Morentin, J. Metwally, A.B. Meyer, G. Milella, A. Mussgiller, L.P. Nair, A. Nürnberg, Y. Otarid, J. Park, D. Pérez Adán, E. Ranken, A. Raspereza, B. Ribeiro Lopes, J. Rübenach, A. Saggio, M. Scham[31,27], S. Schnake[27], P. Schütze, C. Schwanenberger[26], D. Selivanova, M. Shchedrolosiev, R.E. Sosa Ricardo, D. Stafford, F. Vazzoler, A. Ventura Barroso, R. Walsh, Q. Wang, Y. Wen, K. Wichmann, L. Wiens[27], C. Wissing, Y. Yang, A. Zimermmane Castro Santos

University of Hamburg, Hamburg, Germany
A. Albrecht, S. Albrecht, M. Antonello, S. Bein, L. Benato, M. Bonanomi, P. Connor, M. Eich, K. El Morabit, Y. Fischer, A. Fröhlich, C. Garbers, E. Garutti, A. Grohsjean, M. Hajheidari, J. Haller, H.R. Jabusch, G. Kasieczka, P. Keicher, R. Klanner, W. Korcari, T. Kramer, V. Kutzner, F. Labe, J. Lange, A. Lobanov, C. Matthies, A. Mehta, L. Moureaux, M. Mrowietz, A. Nigamova, Y. Nissan, A. Paasch, K.J. Pena Rodriguez, T. Quadfasel, B. Raciti, M. Rieger, D. Savoiu, J. Schindler, P. Schleper, M. Schröder, J. Schwandt, M. Sommerhalder, H. Stadie, G. Steinbrück, A. Tews, M. Wolf

Karlsruher Institut fuer Technologie, Karlsruhe, Germany
S. Brommer, M. Burkart, E. Butz, T. Chwalek, A. Dierlamm, A. Droll, N. Faltermann, M. Giffels, A. Gottmann, F. Hartmann[32], R. Hofsaess, M. Horzela, U. Husemann, J. Kieseler, M. Klute, R. Koppenhöfer, J.M. Lawhorn, M. Link, A. Lintuluoto, S. Maier, S. Mitra, M. Mormile, Th. Müller, M. Neukum, M. Oh, M. Presilla, G. Quast, K. Rabbertz, B. Regnery, N. Shadskiy, I. Shvetsov, H.J. Simonis, N. Trevisani, R. Ulrich, J. van der Linden, R.F. Von Cube, M. Wassmer, S. Wieland, F. Wittig, R. Wolf, S. Wunsch, X. Zuo

Institute of Nuclear and Particle Physics (INPP), NCSR Demokritos, Aghia Paraskevi, Greece

G. Anagnostou, P. Assiouras, G. Daskalakis, A. Kyriakis, A. Papadopoulos[32], A. Stakia

National and Kapodistrian University of Athens, Athens, Greece
P. Kontaxakis, G. Melachroinos, A. Panagiotou, I. Papavergou, I. Paraskevas, N. Saoulidou, K. Theofilatos, E. Tziaferi, K. Vellidis, I. Zisopoulos

National Technical University of Athens, Athens, Greece
G. Bakas, T. Chatzistavrou, G. Karapostoli, K. Kousouris, I. Papakrivopoulos, E. Siamarkou, G. Tsipolitis, A. Zacharopoulou

University of Ioánnina, Ioánnina, Greece
K. Adamidis, I. Bestintzanos, I. Evangelou, C. Foudas, P. Gianneios, C. Kamtsikis, P. Katsoulis, P. Kokkas, P.G. Kosmoglou Kioseoglou, N. Manthos, I. Papadopoulos, J. Strologas

HUN-REN Wigner Research Centre for Physics, Budapest, Hungary
M. Bartók[33], C. Hajdu, D. Horvath[34,35], F. Sikler, V. Veszpremi

MTA-ELTE Lendület CMS Particle and Nuclear Physics Group, Eötvös Loránd University, Budapest, Hungary
M. Csanád, K. Farkas, M.M.A. Gadallah[36], Á. Kadlecsik, P. Major, K. Mandal, G. Pásztor, A.J. Rádl[37], G.I. Veres

Faculty of Informatics, University of Debrecen, Debrecen, Hungary
P. Raics, B. Ujvari[38], G. Zilizi

Institute of Nuclear Research ATOMKI, Debrecen, Hungary
G. Bencze, S. Czellar, J. Karancsi[33], J. Molnar, Z. Szillasi

Karoly Robert Campus, MATE Institute of Technology, Gyongyos, Hungary
T. Csorgo[37], F. Nemes[37], T. Novak

Panjab University, Chandigarh, India
J. Babbar, S. Bansal, S.B. Beri, V. Bhatnagar, G. Chaudhary, S. Chauhan, N. Dhingra[39], A. Kaur, A. Kaur, H. Kaur, M. Kaur, S. Kumar, M. Meena, K. Sandeep, T. Sheokand, J.B. Singh, A. Singla

University of Delhi, Delhi, India
A. Ahmed, A. Bhardwaj, A. Chhetri, B.C. Choudhary, A. Kumar, M. Naimuddin, K. Ranjan, S. Saumya

Saha Institute of Nuclear Physics, HBNI, Kolkata, India
S. Acharya[40], S. Baradia, S. Barman[41], S. Bhattacharya, D. Bhowmik, S. Dutta, S. Dutta, P. Palit, B. Sahu[40], S. Sarkar

Indian Institute of Technology Madras, Madras, India
M.M. Ameen, P.K. Behera, S.C. Behera, S. Chatterjee, P. Jana, P. Kalbhor, J.R. Komaragiri[42], D. Kumar[42], L. Panwar[42], R. Pradhan, P.R. Pujahari, N.R. Saha, A. Sharma, A.K. Sikdar, S. Verma

Tata Institute of Fundamental Research-A, Mumbai, India
T. Aziz, I. Das, S. Dugad, M. Kumar, G.B. Mohanty, P. Suryadevara

Tata Institute of Fundamental Research-B, Mumbai, India
A. Bala, S. Banerjee, R.M. Chatterjee, M. Guchait, Sh. Jain, S. Karmakar, S. Kumar, G. Majumder, K. Mazumdar, S. Mukherjee, S. Parolia, A. Thachayath

National Institute of Science Education and Research, An OCC of Homi Bhabha National Institute, Bhubaneswar, Odisha, India
S. Bahinipati[43], A.K. Das, C. Kar, D. Maity[44], P. Mal, T. Mishra, V.K. Muraleedharan Nair Bindhu[44], K. Naskar[44], A. Nayak[44], P. Sadangi, P. Saha, S.K. Swain, S. Varghese[44], D. Vats[44]

Indian Institute of Science Education and Research (IISER), Pune, India
A. Alpana, S. Dube, B. Gomber[40], B. Kansal, A. Laha, A. Rastogi, S. Sharma

Isfahan University of Technology, Isfahan, Iran
H. Bakhshiansohi[45], E. Khazaie[46], M. Zeinali[47]

Institute for Research in Fundamental Sciences (IPM), Tehran, Iran
S. Chenarani[48], S.M. Etesami, M. Khakzad, M. Mohammadi Najafabadi

University College Dublin, Dublin, Ireland
M. Grunewald

INFN Sezione di Bari[a], Università di Bari[b], Politecnico di Bari[c], Bari, Italy
M. Abbrescia[a,b], R. Aly[a,c,49], A. Colaleo[a,b], D. Creanza[a,c], B. D'Anzi[a,b], N. De Filippis[a,c], M. De Palma[a,b], A. Di Florio[a,c], W. Elmetenawee[a,b,49], L. Fiore[a], G. Iaselli[a,c], M. Louka[a,b], G. Maggi[a,c], M. Maggi[a], I. Margjeka[a,b], V. Mastrapasqua[a,b], S. My[a,b], S. Nuzzo[a,b], A. Pellecchia[a,b], A. Pompili[a,b], G. Pugliese[a,c], R. Radogna[a], G. Ramirez-Sanchez[a,c], D. Ramos[a], A. Ranieri[a], L. Silvestris[a], F.M. Simone[a,b], Ü. Sözbilir[a], A. Stamerra[a], R. Venditti[a], P. Verwilligen[a], A. Zaza[a,b]

INFN Sezione di Bologna[a], Università di Bologna[b], Bologna, Italy
G. Abbiendi[a], C. Battilana[a,b], D. Bonacorsi[a,b], L. Borgonovi[a], R. Campanini[a,b], P. Capiluppi[a,b], A. Castro[a,b], F.R. Cavallo[a], M. Cuffiani[a,b], T. Diotalevi[a,b], F. Fabbri[a], A. Fanfani[a,b], D. Fasanella[a,b], P. Giacomelli[a], L. Giommi[a,b], C. Grandi[a], L. Guiducci[a,b], S. Lo Meo[a,50], L. Lunerti[a,b], S. Marcellini[a], G. Masetti[a], F.L. Navarria[a,b], A. Perrotta[a], F. Primavera[a,b], A.M. Rossi[a,b], T. Rovelli[a,b], G.P. Siroli[a,b]

INFN Sezione di Catania[a], Università di Catania[b], Catania, Italy
S. Costa[a,b,51], A. Di Mattia[a], R. Potenza[a,b], A. Tricomi[a,b,51], C. Tuve[a,b]

INFN Sezione di Firenze[a], Università di Firenze[b], Firenze, Italy
G. Barbagli[a], G. Bardelli[a,b], B. Camaiani[a,b], A. Cassese[a], R. Ceccarelli[a], V. Ciulli[a,b], C. Civinini[a], R. D'Alessandro[a,b], E. Focardi[a,b], T. Kello[a], G. Latino[a,b], P. Lenzi[a,b], M. Lizzo[a], M. Meschini[a], S. Paoletti[a], A. Papanastassiou[a,b], G. Sguazzoni[a], L. Viliani[a]

INFN Laboratori Nazionali di Frascati, Frascati, Italy
L. Benussi, S. Bianco, S. Meola[52], D. Piccolo

INFN Sezione di Genova[a], Università di Genova[b], Genova, Italy
P. Chatagnon[a], F. Ferro[a], E. Robutti[a], S. Tosi[a,b]

INFN Sezione di Milano-Bicocca[a], Università di Milano-Bicocca[b], Milano, Italy
A. Benaglia[a], G. Boldrini[a,b], F. Brivio[a], F. Cetorelli[a], F. De Guio[a,b], M.E. Dinardo[a,b], P. Dini[a], S. Gennai[a], R. Gerosa[a,b], A. Ghezzi[a,b], P. Govoni[a,b], L. Guzzi[a], M.T. Lucchini[a,b], M. Malberti[a], S. Malvezzi[a], A. Massironi[a], D. Menasce[a], L. Moroni[a], M. Paganoni[a,b], D. Pedrini[a], B.S. Pinolini[a], S. Ragazzi[a,b],

T. Tabarelli de Fatis[a,b], D. Zuolo[a]

INFN Sezione di Napoli[a], Università di Napoli 'Federico II'[b], Napoli, Italy; Università della Basilicata[c], Potenza, Italy; Scuola Superiore Meridionale (SSM)[d], Napoli, Italy
S. Buontempo[a], A. Cagnotta[a,b], F. Carnevali[a,b], N. Cavallo[a,c], A. De Iorio[a,b], F. Fabozzi[a,c], A.O.M. Iorio[a,b], L. Lista[a,b,53], P. Paolucci[a,32], B. Rossi[a], C. Sciacca[a,b]

INFN Sezione di Padova[a], Università di Padova[b], Padova, Italy; Università di Trento[c], Trento, Italy
R. Ardino[a], P. Azzi[a], N. Bacchetta[a,54], M. Bellato[a], D. Bisello[a,b], P. Bortignon[a], A. Bragagnolo[a,b], P. Checchia[a], T. Dorigo[a], F. Gasparini[a,b], U. Gasparini[a,b], G. Grosso[a], L. Layer[a,55], E. Lusiani[a], M. Margoni[a,b], A.T. Meneguzzo[a,b], M. Migliorini[a,b], J. Pazzini[a,b], P. Ronchese[a,b], R. Rossin[a,b], F. Simonetto[a,b], G. Strong[a], M. Tosi[a,b], A. Triossi[a,b], S. Ventura[a], H. Yarar[a,b], M. Zanetti[a,b], P. Zotto[a,b], A. Zucchetta[a,b], G. Zumerle[a,b]

INFN Sezione di Pavia[a], Università di Pavia[b], Pavia, Italy
S. Abu Zeid[a,56], C. Aimè[a,b], A. Braghieri[a], S. Calzaferri[a,b], D. Fiorina[a,b], P. Montagna[a,b], V. Re[a], C. Riccardi[a,b], P. Salvini[a], I. Vai[a,b], P. Vitulo[a,b]

INFN Sezione di Perugia[a], Università di Perugia[b], Perugia, Italy
S. Ajmal[a,b], P. Asenov[a,57], G.M. Bilei[a], D. Ciangottini[a,b], L. Fanò[a,b], M. Magherini[a,b], G. Mantovani[a,b], V. Mariani[a,b], M. Menichelli[a], F. Moscatelli[a,57], A. Rossi[a,b], A. Santocchia[a,b], D. Spiga[a], T. Tedeschi[a,b]

INFN Sezione di Pisa[a], Università di Pisa[b], Scuola Normale Superiore di Pisa[c], Pisa, Italy; Università di Siena[d], Siena, Italy
P. Azzurri[a], G. Bagliesi[a], R. Bhattacharya[a], L. Bianchini[a,b], T. Boccali[a], E. Bossini[a], D. Bruschini[a,c], R. Castaldi[a], M.A. Ciocci[a,b], M. Cipriani[a,b], V. D'Amante[a,d], R. Dell'Orso[a], S. Donato[a], A. Giassi[a], F. Ligabue[a,c], D. Matos Figueiredo[a], A. Messineo[a,b], M. Musich[a,b], F. Palla[a], A. Rizzi[a,b], G. Rolandi[a,c], S. Roy Chowdhury[a], T. Sarkar[a], A. Scribano[a], P. Spagnolo[a], R. Tenchini[a], G. Tonelli[a,b], N. Turini[a,d], A. Venturi[a], P.G. Verdini[a]

INFN Sezione di Roma[a], Sapienza Università di Roma[b], Roma, Italy
P. Barria[a], M. Campana[a,b], F. Cavallari[a], L. Cunqueiro Mendez[a,b], D. Del Re[a,b], E. Di Marco[a], M. Diemoz[a], F. Errico[a,b], E. Longo[a,b], P. Meridiani[a], J. Mijuskovic[a,b], G. Organtini[a,b], F. Pandolfi[a], R. Paramatti[a,b], C. Quaranta[a,b], S. Rahatlou[a,b], C. Rovelli[a], F. Santanastasio[a,b], L. Soffi[a]

INFN Sezione di Torino[a], Università di Torino[b], Torino, Italy; Università del Piemonte Orientale[c], Novara, Italy
N. Amapane[a,b], R. Arcidiacono[a,c], S. Argiro[a,b], M. Arneodo[a,c], N. Bartosik[a], R. Bellan[a,b], A. Bellora[a,b], C. Biino[a], N. Cartiglia[a], M. Costa[a,b], R. Covarelli[a,b], N. Demaria[a], L. Finco[a], M. Grippo[a,b], B. Kiani[a,b], F. Legger[a], F. Luongo[a,b], C. Mariotti[a], S. Maselli[a], A. Mecca[a,b], E. Migliore[a,b], M. Monteno[a], R. Mulargia[a], M.M. Obertino[a,b], G. Ortona[a], L. Pacher[a,b], N. Pastrone[a], M. Pelliccioni[a], M. Ruspa[a,c], F. Siviero[a,b], V. Sola[a,b], A. Solano[a,b], D. Soldi[a,b], A. Staiano[a], C. Tarricone[a,b], D. Trocino[a], G. Umoret[a,b], E. Vlasov[a,b]

INFN Sezione di Trieste[a], Università di Trieste[b], Trieste, Italy
S. Belforte[a], V. Candelise[a,b], M. Casarsa[a], F. Cossutti[a], K. De Leo[a,b],

G. Della Ricca[a,b]

Kyungpook National University, Daegu, Korea
S. Dogra, J. Hong, C. Huh, B. Kim, D.H. Kim, J. Kim, H. Lee, S.W. Lee, C.S. Moon, Y.D. Oh, M.S. Ryu, S. Sekmen, Y.C. Yang

Department of Mathematics and Physics - GWNU, Gangneung, Korea
M.S. Kim

Chonnam National University, Institute for Universe and Elementary Particles, Kwangju, Korea
G. Bak, P. Gwak, H. Kim, D.H. Moon

Hanyang University, Seoul, Korea
E. Asilar, D. Kim, T.J. Kim, J.A. Merlin

Korea University, Seoul, Korea
S. Choi, S. Han, B. Hong, K. Lee, K.S. Lee, S. Lee, J. Park, S.K. Park, J. Yoo

Kyung Hee University, Department of Physics, Seoul, Korea
J. Goh

Sejong University, Seoul, Korea
H. S. Kim, Y. Kim, S. Lee

Seoul National University, Seoul, Korea
J. Almond, J.H. Bhyun, J. Choi, W. Jun, J. Kim, J.S. Kim, S. Ko, H. Kwon, H. Lee, J. Lee, J. Lee, B.H. Oh, S.B. Oh, H. Seo, U.K. Yang, I. Yoon

University of Seoul, Seoul, Korea
W. Jang, D.Y. Kang, Y. Kang, S. Kim, B. Ko, J.S.H. Lee, Y. Lee, I.C. Park, Y. Roh, I.J. Watson, S. Yang

Yonsei University, Department of Physics, Seoul, Korea
S. Ha, H.D. Yoo

Sungkyunkwan University, Suwon, Korea
M. Choi, M.R. Kim, H. Lee, Y. Lee, I. Yu

College of Engineering and Technology, American University of the Middle East (AUM), Dasman, Kuwait
T. Beyrouthy, Y. Maghrbi

Riga Technical University, Riga, Latvia
K. Dreimanis, A. Gaile, G. Pikurs, A. Potrebko, M. Seidel, V. Veckalns[58]

University of Latvia (LU), Riga, Latvia
N.R. Strautnieks

Vilnius University, Vilnius, Lithuania
M. Ambrozas, A. Juodagalvis, A. Rinkevicius, G. Tamulaitis

National Centre for Particle Physics, Universiti Malaya, Kuala Lumpur, Malaysia
N. Bin Norjoharuddeen, I. Yusuff[59], Z. Zolkapli

Universidad de Sonora (UNISON), Hermosillo, Mexico
J.F. Benitez, A. Castaneda Hernandez, H.A. Encinas Acosta, L.G. Gallegos Maríñez, M. León Coello, J.A. Murillo Quijada, A. Sehrawat, L. Valencia Palomo

Centro de Investigacion y de Estudios Avanzados del IPN, Mexico City, Mexico
G. Ayala, H. Castilla-Valdez, E. De La Cruz-Burelo, I. Heredia-De La Cruz[60], R. Lopez-Fernandez, C.A. Mondragon Herrera, A. Sánchez Hernández

Universidad Iberoamericana, Mexico City, Mexico
C. Oropeza Barrera, M. Ramírez García

Benemerita Universidad Autonoma de Puebla, Puebla, Mexico
I. Bautista, I. Pedraza, H.A. Salazar Ibarguen, C. Uribe Estrada

University of Montenegro, Podgorica, Montenegro
I. Bubanja, N. Raicevic

University of Canterbury, Christchurch, New Zealand
P.H. Butler

National Centre for Physics, Quaid-I-Azam University, Islamabad, Pakistan
A. Ahmad, M.I. Asghar, A. Awais, M.I.M. Awan, H.R. Hoorani, W.A. Khan

AGH University of Krakow, Faculty of Computer Science, Electronics and Telecommunications, Krakow, Poland
V. Avati, L. Grzanka, M. Malawski

National Centre for Nuclear Research, Swierk, Poland
H. Bialkowska, M. Bluj, B. Boimska, M. Górski, M. Kazana, M. Szleper, P. Zalewski

Institute of Experimental Physics, Faculty of Physics, University of Warsaw, Warsaw, Poland
K. Bunkowski, K. Doroba, A. Kalinowski, M. Konecki, J. Krolikowski, A. Muhammad

Warsaw University of Technology, Warsaw, Poland
K. Pozniak, W. Zabolotny

Laboratório de Instrumentação e Física Experimental de Partículas, Lisboa, Portugal
M. Araujo, D. Bastos, C. Beirão Da Cruz E Silva, A. Boletti, M. Bozzo, T. Camporesi, G. Da Molin, P. Faccioli, M. Gallinaro, J. Hollar, N. Leonardo, T. Niknejad, A. Petrilli, M. Pisano, J. Seixas, J. Varela, J.W. Wulff

Faculty of Physics, University of Belgrade, Belgrade, Serbia
P. Adzic, P. Milenovic

VINCA Institute of Nuclear Sciences, University of Belgrade, Belgrade, Serbia
M. Dordevic, J. Milosevic, V. Rekovic

Centro de Investigaciones Energéticas Medioambientales y Tecnológicas (CIEMAT), Madrid, Spain
M. Aguilar-Benitez, J. Alcaraz Maestre, Cristina F. Bedoya, M. Cepeda, M. Cerrada, N. Colino, B. De La Cruz, A. Delgado Peris, D. Fernández Del Val, J.P. Fernández Ramos, J. Flix, M.C. Fouz, O. Gonzalez Lopez, S. Goy Lopez, J.M. Hernandez, M.I. Josa, J. León Holgado, D. Moran, C. M. Morcillo Perez, Á. Navarro Tobar, C. Perez Dengra, A. Pérez-Calero Yzquierdo, J. Puerta Pelayo, I. Redondo, D.D. Redondo Ferrero, L. Romero, S. Sánchez Navas, L. Urda Gómez, J. Vazquez Escobar, C. Willmott

Universidad Autónoma de Madrid, Madrid, Spain

J.F. de Trocóniz

Universidad de Oviedo, Instituto Universitario de Ciencias y Tecnologías Espaciales de Asturias (ICTEA), Oviedo, Spain
B. Alvarez Gonzalez, J. Cuevas, J. Fernandez Menendez, S. Folgueras, I. Gonzalez Caballero, J.R. González Fernández, E. Palencia Cortezon, C. Ramón Álvarez, V. Rodríguez Bouza, A. Soto Rodríguez, A. Trapote, C. Vico Villalba, P. Vischia

Instituto de Física de Cantabria (IFCA), CSIC-Universidad de Cantabria, Santander, Spain
S. Bhowmik, S. Blanco Fernández, J.A. Brochero Cifuentes, I.J. Cabrillo, A. Calderon, J. Duarte Campderros, M. Fernandez, C. Fernandez Madrazo, G. Gomez, C. Lasaosa García, C. Martinez Rivero, P. Martinez Ruiz del Arbol, F. Matorras, P. Matorras Cuevas, E. Navarrete Ramos, J. Piedra Gomez, L. Scodellaro, I. Vila, J.M. Vizan Garcia

University of Colombo, Colombo, Sri Lanka
M.K. Jayananda, B. Kailasapathy[61], D.U.J. Sonnadara, D.D.C. Wickramarathna

University of Ruhuna, Department of Physics, Matara, Sri Lanka
W.G.D. Dharmaratna[62], K. Liyanage, N. Perera, N. Wickramage

CERN, European Organization for Nuclear Research, Geneva, Switzerland
D. Abbaneo, C. Amendola, E. Auffray, G. Auzinger, J. Baechler, D. Barney, A. Bermúdez Martínez, M. Bianco, B. Bilin, A.A. Bin Anuar, A. Bocci, E. Brondolin, C. Caillol, G. Cerminara, N. Chernyavskaya, D. d'Enterria, A. Dabrowski, A. David, A. De Roeck, M.M. Defranchis, M. Deile, M. Dobson, F. Fallavollita[63], L. Forthomme, G. Franzoni, W. Funk, S. Giani, D. Gigi, K. Gill, F. Glege, L. Gouskos, M. Haranko, J. Hegeman, B. Huber, V. Innocente, T. James, P. Janot, S. Laurila, P. Lecoq, E. Leutgeb, C. Lourenço, B. Maier, L. Malgeri, M. Mannelli, A.C. Marini, M. Matthewman, F. Meijers, S. Mersi, E. Meschi, V. Milosevic, F. Moortgat, M. Mulders, S. Orfanelli, F. Pantaleo, G. Petrucciani, A. Pfeiffer, M. Pierini, D. Piparo, H. Qu, D. Rabady, G. Reales Gutiérrez, M. Rovere, H. Sakulin, S. Scarfi, C. Schwick, M. Selvaggi, A. Sharma, K. Shchelina, P. Silva, P. Sphicas[64], A.G. Stahl Leiton, A. Steen, S. Summers, D. Treille, P. Tropea, A. Tsirou, D. Walter, J. Wanczyk[65], K.A. Wozniak[66], S. Wuchterl, P. Zehetner, P. Zejdl, W.D. Zeuner

Paul Scherrer Institut, Villigen, Switzerland
T. Bevilacqua[67], L. Caminada[67], A. Ebrahimi, W. Erdmann, R. Horisberger, Q. Ingram, H.C. Kaestli, D. Kotlinski, C. Lange, M. Missiroli[67], L. Noehte[67], T. Rohe

ETH Zurich - Institute for Particle Physics and Astrophysics (IPA), Zurich, Switzerland
T.K. Aarrestad, K. Androsov[65], M. Backhaus, A. Calandri, C. Cazzaniga, K. Datta, A. De Cosa, G. Dissertori, M. Dittmar, M. Donegà, F. Eble, M. Galli, K. Gedia, F. Glessgen, C. Grab, D. Hits, W. Lustermann, A.-M. Lyon, R.A. Manzoni, M. Marchegiani, L. Marchese, C. Martin Perez, A. Mascellani[65], F. Nessi-Tedaldi, F. Pauss, V. Perovic, S. Pigazzini, M.G. Ratti, M. Reichmann, C. Reissel, T. Reitenspiess, B. Ristic, F. Riti, D. Ruini, D.A. Sanz Becerra, R. Seidita, J. Steggemann[65], D. Valsecchi, R. Wallny

Universität Zürich, Zurich, Switzerland
C. Amsler[68], P. Bärtschi, C. Botta, D. Brzhechko, M.F. Canelli, K. Cormier,

R. Del Burgo, J.K. Heikkilä, M. Huwiler, W. Jin, A. Jofrehei, B. Kilminster, S. Leontsinis, S.P. Liechti, A. Macchiolo, P. Meiring, V.M. Mikuni, U. Molinatti, I. Neutelings, A. Reimers, P. Robmann, S. Sanchez Cruz, K. Schweiger, M. Senger, Y. Takahashi, R. Tramontano

National Central University, Chung-Li, Taiwan
C. Adloff[69], C.M. Kuo, W. Lin, P.K. Rout, P.C. Tiwari[42], S.S. Yu

National Taiwan University (NTU), Taipei, Taiwan
L. Ceard, Y. Chao, K.F. Chen, P.s. Chen, Z.g. Chen, W.-S. Hou, T.h. Hsu, Y.w. Kao, R. Khurana, G. Kole, Y.y. Li, R.-S. Lu, E. Paganis, A. Psallidas, X.f. Su, J. Thomas-Wilsker, L.s. Tsai, H.y. Wu, E. Yazgan

High Energy Physics Research Unit, Department of Physics, Faculty of Science, Chulalongkorn University, Bangkok, Thailand
C. Asawatangtrakuldee, N. Srimanobhas, V. Wachirapusitanand

Çukurova University, Physics Department, Science and Art Faculty, Adana, Turkey
D. Agyel, F. Boran, Z.S. Demiroglu, F. Dolek, I. Dumanoglu[70], E. Eskut, Y. Guler[71], E. Gurpinar Guler[71], C. Isik, O. Kara, A. Kayis Topaksu, U. Kiminsu, G. Onengut, K. Ozdemir[72], A. Polatoz, B. Tali[73], U.G. Tok, S. Turkcapar, E. Uslan, I.S. Zorbakir

Middle East Technical University, Physics Department, Ankara, Turkey
M. Yalvac[74]

Bogazici University, Istanbul, Turkey
B. Akgun, I.O. Atakisi, E. Gülmez, M. Kaya[75], O. Kaya[76], S. Tekten[77]

Istanbul Technical University, Istanbul, Turkey
A. Cakir, K. Cankocak[70,78], Y. Komurcu, S. Sen[79]

Istanbul University, Istanbul, Turkey
O. Aydilek, S. Cerci[73], V. Epshteyn, B. Hacisahinoglu, I. Hos[80], B. Isildak[81], B. Kaynak, S. Ozkorucuklu, O. Potok, H. Sert, C. Simsek, D. Sunar Cerci[73], C. Zorbilmez

Institute for Scintillation Materials of National Academy of Science of Ukraine, Kharkiv, Ukraine
A. Boyaryntsev, B. Grynyov

National Science Centre, Kharkiv Institute of Physics and Technology, Kharkiv, Ukraine
L. Levchuk

University of Bristol, Bristol, United Kingdom
D. Anthony, J.J. Brooke, A. Bundock, F. Bury, E. Clement, D. Cussans, H. Flacher, M. Glowacki, J. Goldstein, H.F. Heath, L. Kreczko, B. Krikler, S. Paramesvaran, S. Seif El Nasr-Storey, V.J. Smith, N. Stylianou[82], K. Walkingshaw Pass, R. White

Rutherford Appleton Laboratory, Didcot, United Kingdom
A.H. Ball, K.W. Bell, A. Belyaev[83], C. Brew, R.M. Brown, D.J.A. Cockerill, C. Cooke, K.V. Ellis, K. Harder, S. Harper, M.-L. Holmberg[84], J. Linacre, K. Manolopoulos, D.M. Newbold, E. Olaiya, D. Petyt, T. Reis, G. Salvi, T. Schuh, C.H. Shepherd-Themistocleous, I.R. Tomalin, T. Williams

Imperial College, London, United Kingdom
R. Bainbridge, P. Bloch, C.E. Brown, O. Buchmuller, V. Cacchio, C.A. Carrillo Montoya, G.S. Chahal[85], D. Colling, J.S. Dancu, P. Dauncey, G. Davies, J. Davies, M. Della Negra, S. Fayer, G. Fedi, G. Hall, M.H. Hassanshahi, A. Howard, G. Iles, M. Knight, J. Langford, L. Lyons, A.-M. Magnan, S. Malik, A. Martelli, M. Mieskolainen, J. Nash[86], M. Pesaresi, B.C. Radburn-Smith, A. Richards, A. Rose, C. Seez, R. Shukla, A. Tapper, K. Uchida, G.P. Uttley, L.H. Vage, T. Virdee[32], M. Vojinovic, N. Wardle, D. Winterbottom

Brunel University, Uxbridge, United Kingdom
K. Coldham, J.E. Cole, A. Khan, P. Kyberd, I.D. Reid

Baylor University, Waco, Texas, USA
S. Abdullin, A. Brinkerhoff, B. Caraway, J. Dittmann, K. Hatakeyama, J. Hiltbrand, A.R. Kanuganti, B. McMaster, M. Saunders, S. Sawant, C. Sutantawibul, M. Toms[87], J. Wilson

Catholic University of America, Washington, DC, USA
R. Bartek, A. Dominguez, C. Huerta Escamilla, A.E. Simsek, R. Uniyal, A.M. Vargas Hernandez

The University of Alabama, Tuscaloosa, Alabama, USA
R. Chudasama, S.I. Cooper, S.V. Gleyzer, C.U. Perez, P. Rumerio[88], E. Usai, C. West, R. Yi

Boston University, Boston, Massachusetts, USA
A. Akpinar, A. Albert, D. Arcaro, C. Cosby, Z. Demiragli, C. Erice, E. Fontanesi, D. Gastler, S. Jeon, J. Rohlf, K. Salyer, D. Sperka, D. Spitzbart, I. Suarez, A. Tsatsos, S. Yuan

Brown University, Providence, Rhode Island, USA
G. Benelli, X. Coubez[27], D. Cutts, M. Hadley, U. Heintz, J.M. Hogan[89], T. Kwon, G. Landsberg, K.T. Lau, D. Li, J. Luo, S. Mondal, M. Narain[†], N. Pervan, S. Sagir[90], F. Simpson, M. Stamenkovic, W.Y. Wong, X. Yan, W. Zhang

University of California, Davis, Davis, California, USA
S. Abbott, J. Bonilla, C. Brainerd, R. Breedon, M. Calderon De La Barca Sanchez, M. Chertok, M. Citron, J. Conway, P.T. Cox, R. Erbacher, F. Jensen, O. Kukral, G. Mocellin, M. Mulhearn, D. Pellett, W. Wei, Y. Yao, F. Zhang

University of California, Los Angeles, California, USA
M. Bachtis, R. Cousins, A. Datta, J. Hauser, M. Ignatenko, M.A. Iqbal, T. Lam, E. Manca, D. Saltzberg, V. Valuev

University of California, Riverside, Riverside, California, USA
R. Clare, J.W. Gary, M. Gordon, G. Hanson, W. Si, S. Wimpenny[†]

University of California, San Diego, La Jolla, California, USA
J.G. Branson, S. Cittolin, S. Cooperstein, D. Diaz, J. Duarte, L. Giannini, J. Guiang, R. Kansal, V. Krutelyov, R. Lee, J. Letts, M. Masciovecchio, F. Mokhtar, M. Pieri, M. Quinnan, B.V. Sathia Narayanan, V. Sharma, M. Tadel, E. Vourliotis, F. Würthwein, Y. Xiang, A. Yagil

University of California, Santa Barbara - Department of Physics, Santa Barbara, California, USA

A. Barzdukas, L. Brennan, C. Campagnari, G. Collura, A. Dorsett, J. Incandela, M. Kilpatrick, J. Kim, A.J. Li, P. Masterson, H. Mei, M. Oshiro, J. Richman, U. Sarica, R. Schmitz, F. Setti, J. Sheplock, D. Stuart, S. Wang

California Institute of Technology, Pasadena, California, USA
A. Bornheim, O. Cerri, A. Latorre, J. Mao, H.B. Newman, T. Q. Nguyen, M. Spiropulu, J.R. Vlimant, C. Wang, S. Xie, R.Y. Zhu

Carnegie Mellon University, Pittsburgh, Pennsylvania, USA
J. Alison, S. An, M.B. Andrews, P. Bryant, V. Dutta, T. Ferguson, A. Harilal, C. Liu, T. Mudholkar, S. Murthy, M. Paulini, A. Roberts, A. Sanchez, W. Terrill

University of Colorado Boulder, Boulder, Colorado, USA
J.P. Cumalat, W.T. Ford, A. Hassani, G. Karathanasis, E. MacDonald, N. Manganelli, F. Marini, A. Perloff, C. Savard, N. Schonbeck, K. Stenson, K.A. Ulmer, S.R. Wagner, N. Zipper

Cornell University, Ithaca, New York, USA
J. Alexander, S. Bright-Thonney, X. Chen, D.J. Cranshaw, J. Fan, X. Fan, D. Gadkari, S. Hogan, J. Monroy, J.R. Patterson, J. Reichert, M. Reid, A. Ryd, J. Thom, P. Wittich, R. Zou

Fermi National Accelerator Laboratory, Batavia, Illinois, USA
M. Albrow, M. Alyari, O. Amram, G. Apollinari, A. Apresyan, L.A.T. Bauerdick, D. Berry, J. Berryhill, P.C. Bhat, K. Burkett, J.N. Butler, A. Canepa, G.B. Cerati, H.W.K. Cheung, F. Chlebana, G. Cummings, J. Dickinson, I. Dutta, V.D. Elvira, Y. Feng, J. Freeman, A. Gandrakota, Z. Gecse, L. Gray, D. Green, A. Grummer, S. Grünendahl, D. Guerrero, O. Gutsche, R.M. Harris, R. Heller, T.C. Herwig, J. Hirschauer, L. Horyn, B. Jayatilaka, S. Jindariani, M. Johnson, U. Joshi, T. Klijnsma, B. Klima, K.H.M. Kwok, S. Lammel, D. Lincoln, R. Lipton, T. Liu, C. Madrid, K. Maeshima, C. Mantilla, D. Mason, P. McBride, P. Merkel, S. Mrenna, S. Nahn, J. Ngadiuba, D. Noonan, V. Papadimitriou, N. Pastika, K. Pedro, C. Pena[91], F. Ravera, A. Reinsvold Hall[92], L. Ristori, E. Sexton-Kennedy, N. Smith, A. Soha, L. Spiegel, S. Stoynev, J. Strait, L. Taylor, S. Tkaczyk, N.V. Tran, L. Uplegger, E.W. Vaandering, I. Zoi

University of Florida, Gainesville, Florida, USA
C. Aruta, P. Avery, D. Bourilkov, L. Cadamuro, P. Chang, V. Cherepanov, R.D. Field, E. Koenig, M. Kolosova, J. Konigsberg, A. Korytov, K.H. Lo, K. Matchev, N. Menendez, G. Mitselmakher, K. Mohrman, A. Muthirakalayil Madhu, N. Rawal, D. Rosenzweig, S. Rosenzweig, K. Shi, J. Wang

Florida State University, Tallahassee, Florida, USA
T. Adams, A. Al Kadhim, A. Askew, N. Bower, R. Habibullah, V. Hagopian, R. Hashmi, R.S. Kim, S. Kim, T. Kolberg, G. Martinez, H. Prosper, P.R. Prova, O. Viazlo, M. Wulansatiti, R. Yohay, J. Zhang

Florida Institute of Technology, Melbourne, Florida, USA
B. Alsufyani, M.M. Baarmand, S. Butalla, T. Elkafrawy[56], M. Hohlmann, R. Kumar Verma, M. Rahmani

University of Illinois Chicago, Chicago, USA, Chicago, USA
M.R. Adams, C. Bennett, R. Cavanaugh, S. Dittmer, R. Escobar Franco, O. Evdoki-

mov, C.E. Gerber, D.J. Hofman, J.h. Lee, D. S. Lemos, A.H. Merrit, C. Mills, S. Nanda, G. Oh, B. Ozek, D. Pilipovic, T. Roy, S. Rudrabhatla, M.B. Tonjes, N. Varelas, X. Wang, Z. Ye, J. Yoo

The University of Iowa, Iowa City, Iowa, USA
M. Alhusseini, D. Blend, K. Dilsiz[93], L. Emediato, G. Karaman, O.K. Köseyan, J.-P. Merlo, A. Mestvirishvili[94], J. Nachtman, O. Neogi, H. Ogul[95], Y. Onel, A. Penzo, C. Snyder, E. Tiras[96]

Johns Hopkins University, Baltimore, Maryland, USA
B. Blumenfeld, L. Corcodilos, J. Davis, A.V. Gritsan, L. Kang, S. Kyriacou, P. Maksimovic, M. Roguljic, J. Roskes, S. Sekhar, M. Swartz, T.Á. Vámi

The University of Kansas, Lawrence, Kansas, USA
A. Abreu, L.F. Alcerro Alcerro, J. Anguiano, P. Baringer, A. Bean, Z. Flowers, D. Grove, J. King, G. Krintiras, M. Lazarovits, C. Le Mahieu, C. Lindsey, J. Marquez, N. Minafra, M. Murray, M. Nickel, M. Pitt, S. Popescu[97], C. Rogan, C. Royon, R. Salvatico, S. Sanders, C. Smith, Q. Wang, G. Wilson

Kansas State University, Manhattan, Kansas, USA
B. Allmond, A. Ivanov, K. Kaadze, A. Kalogeropoulos, D. Kim, Y. Maravin, K. Nam, J. Natoli, D. Roy, G. Sorrentino

Lawrence Livermore National Laboratory, Livermore, California, USA
F. Rebassoo, D. Wright

University of Maryland, College Park, Maryland, USA
A. Baden, A. Belloni, A. Bethani, Y.M. Chen, S.C. Eno, N.J. Hadley, S. Jabeen, R.G. Kellogg, T. Koeth, Y. Lai, S. Lascio, A.C. Mignerey, S. Nabili, C. Palmer, C. Papageorgakis, M.M. Paranjpe, L. Wang

Massachusetts Institute of Technology, Cambridge, Massachusetts, USA
J. Bendavid, W. Busza, I.A. Cali, Y. Chen, M. D'Alfonso, J. Eysermans, C. Freer, G. Gomez-Ceballos, M. Goncharov, P. Harris, D. Hoang, D. Kovalskyi, J. Krupa, L. Lavezzo, Y.-J. Lee, K. Long, C. Mironov, C. Paus, D. Rankin, C. Roland, G. Roland, S. Rothman, Z. Shi, G.S.F. Stephans, J. Wang, Z. Wang, B. Wyslouch, T. J. Yang

University of Minnesota, Minneapolis, Minnesota, USA
B. Crossman, B.M. Joshi, C. Kapsiak, M. Krohn, D. Mahon, J. Mans, B. Marzocchi, S. Pandey, M. Revering, R. Rusack, R. Saradhy, N. Schroeder, N. Strobbe, M.A. Wadud

University of Mississippi, Oxford, Mississippi, USA
L.M. Cremaldi

University of Nebraska-Lincoln, Lincoln, Nebraska, USA
K. Bloom, M. Bryson, D.R. Claes, C. Fangmeier, F. Golf, G. Haza, J. Hossain, C. Joo, I. Kravchenko, I. Reed, J.E. Siado, W. Tabb, A. Vagnerini, A. Wightman, F. Yan, D. Yu, A.G. Zecchinelli

State University of New York at Buffalo, Buffalo, New York, USA
G. Agarwal, H. Bandyopadhyay, L. Hay, I. Iashvili, A. Kharchilava, M. Morris, D. Nguyen, S. Rappoccio, H. Rejeb Sfar, A. Williams

Northeastern University, Boston, Massachusetts, USA
E. Barberis, Y. Haddad, Y. Han, A. Krishna, J. Li, M. Lu, G. Madigan, R. Mccarthy, D.M. Morse, V. Nguyen, T. Orimoto, A. Parker, L. Skinnari, A. Tishelman-Charny, B. Wang, D. Wood

Northwestern University, Evanston, Illinois, USA
S. Bhattacharya, J. Bueghly, Z. Chen, K.A. Hahn, Y. Liu, Y. Miao, D.G. Monk, M.H. Schmitt, A. Taliercio, M. Velasco

University of Notre Dame, Notre Dame, Indiana, USA
R. Band, R. Bucci, S. Castells, M. Cremonesi, A. Das, R. Goldouzian, M. Hildreth, K.W. Ho, K. Hurtado Anampa, T. Ivanov, C. Jessop, K. Lannon, J. Lawrence, N. Loukas, L. Lutton, J. Mariano, N. Marinelli, I. Mcalister, T. McCauley, C. Mcgrady, C. Moore, Y. Musienko[17], H. Nelson, M. Osherson, A. Piccinelli, R. Ruchti, A. Townsend, Y. Wan, M. Wayne, H. Yockey, M. Zarucki, L. Zygala

The Ohio State University, Columbus, Ohio, USA
A. Basnet, B. Bylsma, M. Carrigan, L.S. Durkin, C. Hill, M. Joyce, A. Lesauvage, M. Nunez Ornelas, K. Wei, B.L. Winer, B. R. Yates

Princeton University, Princeton, New Jersey, USA
F.M. Addesa, H. Bouchamaoui, P. Das, G. Dezoort, P. Elmer, A. Frankenthal, B. Greenberg, N. Haubrich, S. Higginbotham, G. Kopp, S. Kwan, D. Lange, A. Loeliger, D. Marlow, I. Ojalvo, J. Olsen, A. Shevelev, D. Stickland, C. Tully

University of Puerto Rico, Mayaguez, Puerto Rico, USA
S. Malik

Purdue University, West Lafayette, Indiana, USA
A.S. Bakshi, V.E. Barnes, S. Chandra, R. Chawla, S. Das, A. Gu, L. Gutay, M. Jones, A.W. Jung, D. Kondratyev, A.M. Koshy, M. Liu, G. Negro, N. Neumeister, G. Paspalaki, S. Piperov, V. Scheurer, J.F. Schulte, M. Stojanovic, J. Thieman, A. K. Virdi, F. Wang, W. Xie

Purdue University Northwest, Hammond, Indiana, USA
J. Dolen, N. Parashar, A. Pathak

Rice University, Houston, Texas, USA
D. Acosta, A. Baty, T. Carnahan, K.M. Ecklund, P.J. Fernández Manteca, S. Freed, P. Gardner, F.J.M. Geurts, A. Kumar, W. Li, O. Miguel Colin, B.P. Padley, R. Redjimi, J. Rotter, E. Yigitbasi, Y. Zhang

University of Rochester, Rochester, New York, USA
A. Bodek, P. de Barbaro, R. Demina, J.L. Dulemba, C. Fallon, A. Garcia-Bellido, O. Hindrichs, A. Khukhunaishvili, P. Parygin[87], E. Popova[87], R. Taus, G.P. Van Onsem

The Rockefeller University, New York, New York, USA
K. Goulianos

Rutgers, The State University of New Jersey, Piscataway, New Jersey, USA
B. Chiarito, J.P. Chou, Y. Gershtein, E. Halkiadakis, A. Hart, M. Heindl, D. Jaroslawski, O. Karacheban[30], I. Laflotte, A. Lath, R. Montalvo, K. Nash, H. Routray, S. Salur, S. Schnetzer, S. Somalwar, R. Stone, S.A. Thayil, S. Thomas, J. Vora, H. Wang

University of Tennessee, Knoxville, Tennessee, USA
H. Acharya, D. Ally, A.G. Delannoy, S. Fiorendi, T. Holmes, N. Karunarathna, L. Lee, E. Nibigira, S. Spanier

Texas A&M University, College Station, Texas, USA
D. Aebi, M. Ahmad, O. Bouhali[98], M. Dalchenko, R. Eusebi, J. Gilmore, T. Huang, T. Kamon[99], H. Kim, S. Luo, S. Malhotra, R. Mueller, D. Overton, D. Rathjens, A. Safonov

Texas Tech University, Lubbock, Texas, USA
N. Akchurin, J. Damgov, V. Hegde, A. Hussain, Y. Kazhykarim, K. Lamichhane, S.W. Lee, A. Mankel, T. Mengke, S. Muthumuni, T. Peltola, I. Volobouev, A. Whitbeck

Vanderbilt University, Nashville, Tennessee, USA
E. Appelt, S. Greene, A. Gurrola, W. Johns, R. Kunnawalkam Elayavalli, A. Melo, F. Romeo, P. Sheldon, S. Tuo, J. Velkovska, J. Viinikainen

University of Virginia, Charlottesville, Virginia, USA
B. Cardwell, B. Cox, J. Hakala, R. Hirosky, A. Ledovskoy, C. Neu, C.E. Perez Lara

Wayne State University, Detroit, Michigan, USA
P.E. Karchin

University of Wisconsin - Madison, Madison, Wisconsin, USA
A. Aravind, S. Banerjee, K. Black, T. Bose, S. Dasu, I. De Bruyn, P. Everaerts, C. Galloni, H. He, M. Herndon, A. Herve, C.K. Koraka, A. Lanaro, R. Loveless, J. Madhusudanan Sreekala, A. Mallampalli, A. Mohammadi, S. Mondal, G. Parida, D. Pinna, A. Savin, V. Shang, V. Sharma, W.H. Smith, D. Teague, H.F. Tsoi, W. Vetens, A. Warden

Authors affiliated with an institute or an international laboratory covered by a cooperation agreement with CERN
S. Afanasiev, V. Andreev, Yu. Andreev, T. Aushev, M. Azarkin, I. Azhgirey, A. Babaev, A. Belyaev, V. Blinov[100], E. Boos, V. Borshch, D. Budkouski, V. Bunichev, V. Chekhovsky, R. Chistov[100], M. Danilov[100], A. Dermenev, T. Dimova[100], D. Druzhkin[101], M. Dubinin[91], L. Dudko, G. Gavrilov, V. Gavrilov, S. Gninenko, V. Golovtcov, N. Golubev, I. Golutvin, I. Gorbunov, Y. Ivanov, V. Kachanov, L. Kardapoltsev[100], V. Karjavine, A. Karneyeu, V. Kim[100], M. Kirakosyan, D. Kirpichnikov, M. Kirsanov, V. Klyukhin, O. Kodolova[102], D. Konstantinov, V. Korenkov, A. Kozyrev[100], N. Krasnikov, A. Lanev, P. Levchenko[103], N. Lychkovskaya, V. Makarenko, A. Malakhov, V. Matveev[100], V. Murzin, A. Nikitenko[104,102], S. Obraztsov, V. Oreshkin, V. Palichik, V. Perelygin, M. Perfilov, S. Petrushanko, S. Polikarpov[100], V. Popov, O. Radchenko[100], R. Ryutin, M. Savina, V. Savrin, V. Shalaev, S. Shmatov, S. Shulha, Y. Skovpen[100], S. Slabospitskii, V. Smirnov, A. Snigirev, D. Sosnov, V. Sulimov, E. Tcherniaev, A. Terkulov, O. Teryaev, I. Tlisova, A. Toropin, L. Uvarov, A. Uzunian, A. Volkov, A. Vorobyev†, G. Vorotnikov, N. Voytishin, B.S. Yuldashev[105], A. Zarubin, I. Zhizhin, A. Zhokin

†: Deceased
[1]Also at Yerevan State University, Yerevan, Armenia
[2]Also at TU Wien, Vienna, Austria

[3]Also at Institute of Basic and Applied Sciences, Faculty of Engineering, Arab Academy for Science, Technology and Maritime Transport, Alexandria, Egypt
[4]Also at Ghent University, Ghent, Belgium
[5]Also at Universidade Estadual de Campinas, Campinas, Brazil
[6]Also at Federal University of Rio Grande do Sul, Porto Alegre, Brazil
[7]Also at UFMS, Nova Andradina, Brazil
[8]Also at Nanjing Normal University, Nanjing, China
[9]Now at Henan Normal University, Xinxiang, China
[10]Now at The University of Iowa, Iowa City, Iowa, USA
[11]Also at University of Chinese Academy of Sciences, Beijing, China
[12]Also at China Center of Advanced Science and Technology, Beijing, China
[13]Also at University of Chinese Academy of Sciences, Beijing, China
[14]Also at China Spallation Neutron Source, Guangdong, China
[15]Also at Université Libre de Bruxelles, Bruxelles, Belgium
[16]Also at University of Latvia (LU), Riga, Latvia
[17]Also at an institute or an international laboratory covered by a cooperation agreement with CERN
[18]Also at Suez University, Suez, Egypt
[19]Now at British University in Egypt, Cairo, Egypt
[20]Also at Birla Institute of Technology, Mesra, Mesra, India
[21]Also at Purdue University, West Lafayette, Indiana, USA
[22]Also at Université de Haute Alsace, Mulhouse, France
[23]Also at Istinye University, Istanbul, Turkey
[24]Also at The University of the State of Amazonas, Manaus, Brazil
[25]Also at Erzincan Binali Yildirim University, Erzincan, Turkey
[26]Also at University of Hamburg, Hamburg, Germany
[27]Also at RWTH Aachen University, III. Physikalisches Institut A, Aachen, Germany
[28]Also at Isfahan University of Technology, Isfahan, Iran
[29]Also at Bergische University Wuppertal (BUW), Wuppertal, Germany
[30]Also at Brandenburg University of Technology, Cottbus, Germany
[31]Also at Forschungszentrum Jülich, Juelich, Germany
[32]Also at CERN, European Organization for Nuclear Research, Geneva, Switzerland
[33]Also at Institute of Physics, University of Debrecen, Debrecen, Hungary
[34]Also at Institute of Nuclear Research ATOMKI, Debrecen, Hungary
[35]Now at Universitatea Babes-Bolyai - Facultatea de Fizica, Cluj-Napoca, Romania
[36]Also at Physics Department, Faculty of Science, Assiut University, Assiut, Egypt
[37]Also at HUN-REN Wigner Research Centre for Physics, Budapest, Hungary
[38]Also at Faculty of Informatics, University of Debrecen, Debrecen, Hungary
[39]Also at Punjab Agricultural University, Ludhiana, India
[40]Also at University of Hyderabad, Hyderabad, India
[41]Also at University of Visva-Bharati, Santiniketan, India
[42]Also at Indian Institute of Science (IISc), Bangalore, India
[43]Also at IIT Bhubaneswar, Bhubaneswar, India
[44]Also at Institute of Physics, Bhubaneswar, India
[45]Also at Deutsches Elektronen-Synchrotron, Hamburg, Germany
[46]Also at Department of Physics, Isfahan University of Technology, Isfahan, Iran
[47]Also at Sharif University of Technology, Tehran, Iran
[48]Also at Department of Physics, University of Science and Technology of Mazandaran, Behshahr, Iran

[49]Also at Helwan University, Cairo, Egypt
[50]Also at Italian National Agency for New Technologies, Energy and Sustainable Economic Development, Bologna, Italy
[51]Also at Centro Siciliano di Fisica Nucleare e di Struttura Della Materia, Catania, Italy
[52]Also at Università degli Studi Guglielmo Marconi, Roma, Italy
[53]Also at Scuola Superiore Meridionale, Università di Napoli 'Federico II', Napoli, Italy
[54]Also at Fermi National Accelerator Laboratory, Batavia, Illinois, USA
[55]Also at Università di Napoli 'Federico II', Napoli, Italy
[56]Also at Ain Shams University, Cairo, Egypt
[57]Also at Consiglio Nazionale delle Ricerche - Istituto Officina dei Materiali, Perugia, Italy
[58]Also at Riga Technical University, Riga, Latvia
[59]Also at Department of Applied Physics, Faculty of Science and Technology, Universiti Kebangsaan Malaysia, Bangi, Malaysia
[60]Also at Consejo Nacional de Ciencia y Tecnología, Mexico City, Mexico
[61]Also at Trincomalee Campus, Eastern University, Sri Lanka, Nilaveli, Sri Lanka
[62]Also at Saegis Campus, Nugegoda, Sri Lanka
[63]Also at INFN Sezione di Pavia, Università di Pavia, Pavia, Italy
[64]Also at National and Kapodistrian University of Athens, Athens, Greece
[65]Also at Ecole Polytechnique Fédérale Lausanne, Lausanne, Switzerland
[66]Also at University of Vienna, Vienna, Austria
[67]Also at Universität Zürich, Zurich, Switzerland
[68]Also at Stefan Meyer Institute for Subatomic Physics, Vienna, Austria
[69]Also at Laboratoire d'Annecy-le-Vieux de Physique des Particules, IN2P3-CNRS, Annecy-le-Vieux, France
[70]Also at Near East University, Research Center of Experimental Health Science, Mersin, Turkey
[71]Also at Konya Technical University, Konya, Turkey
[72]Also at Izmir Bakircay University, Izmir, Turkey
[73]Also at Adiyaman University, Adiyaman, Turkey
[74]Also at Bozok Universitetesi Rektörlügü, Yozgat, Turkey
[75]Also at Marmara University, Istanbul, Turkey
[76]Also at Milli Savunma University, Istanbul, Turkey
[77]Also at Kafkas University, Kars, Turkey
[78]Now at Istanbul Okan University, Istanbul, Turkey
[79]Also at Hacettepe University, Ankara, Turkey
[80]Also at Istanbul University - Cerrahpasa, Faculty of Engineering, Istanbul, Turkey
[81]Also at Yildiz Technical University, Istanbul, Turkey
[82]Also at Vrije Universiteit Brussel, Brussel, Belgium
[83]Also at School of Physics and Astronomy, University of Southampton, Southampton, United Kingdom
[84]Also at University of Bristol, Bristol, United Kingdom
[85]Also at IPPP Durham University, Durham, United Kingdom
[86]Also at Monash University, Faculty of Science, Clayton, Australia
[87]Now at an institute or an international laboratory covered by a cooperation agreement with CERN
[88]Also at Università di Torino, Torino, Italy
[89]Also at Bethel University, St. Paul, Minnesota, USA
[90]Also at Karamanoğlu Mehmetbey University, Karaman, Turkey
[91]Also at California Institute of Technology, Pasadena, California, USA

[92]Also at United States Naval Academy, Annapolis, Maryland, USA
[93]Also at Bingol University, Bingol, Turkey
[94]Also at Georgian Technical University, Tbilisi, Georgia
[95]Also at Sinop University, Sinop, Turkey
[96]Also at Erciyes University, Kayseri, Turkey
[97]Also at Horia Hulubei National Institute of Physics and Nuclear Engineering (IFIN-HH), Bucharest, Romania
[98]Also at Texas A&M University at Qatar, Doha, Qatar
[99]Also at Kyungpook National University, Daegu, Korea
[100]Also at another institute or international laboratory covered by a cooperation agreement with CERN
[101]Also at Universiteit Antwerpen, Antwerpen, Belgium
[102]Also at Yerevan Physics Institute, Yerevan, Armenia
[103]Also at Northeastern University, Boston, Massachusetts, USA
[104]Also at Imperial College, London, United Kingdom
[105]Also at Institute of Nuclear Physics of the Uzbekistan Academy of Sciences, Tashkent, Uzbekistan